5-2010

Gas-Assisted Powder Injection Molding: A Comparison of Residual Wall Thickness Between Metal Cavity vs. SLA Cavity and Effect of Mold Temperature on Residual Wall Thickness

Donghan Kim
University of Texas-Pan American

GAS-ASSISTED POWDER INJECTION MOLDING: A COMPARISON OF RESIDUAL WALL THICKNESS BETWEEN METAL CAVITY VS. SLA CAVITY AND EFFECT OF MOLD TEMPERATURE ON RESIDUAL WALL THICKNESS

A Thesis

by

DONGHAN KIM

Submitted to the Graduate School of the
University of Texas-Pan American
In partial fulfillment of the requirements for the degree of

MASTER OF SCIENCE

May 2010

Major Subject: Manufacturing Engineering

GAS-ASSISTED POWDER INJECTION MOLDING: A COMPARISON OF RESIDUAL WALL THICKNESS BETWEEN METAL CAVITY VS. SLA CAVITY AND EFFECT OF MOLD TEMPERATURE ON RESIDUAL WALL THICKNESS

A Thesis
by
DONGHAN KIM

COMMITTEE MEMBERS

Dr. Kye Hwan Lee
Chair of the Committee

Dr. Seokyoung Ahn
Committee Member

Dr. Rajiv Nambiar
Committee Member

Dr. Miguel A. Gonzalez
Committee Member

Dr. Douglas H. Timmer
Committee Member

May 2010

ABSTRACT

Kim, Donghan, Gas-Assisted Powder Injection Molding: A Comparison of Residual Wall Thickness Between Metal Cavity vs. SLA Cavity and Effect of Mold Temperature on Residual Wall Thickness. Master of Science (MS), May, 2010, 65 pp., 12 Tables, 34 figures, 37 references, 33 titles.

The effects of processing variables on gas penetration depth and Residual Wall Thickness (RWT) in an aluminum (Al) cavity of Gas-Assisted Injection Molding (GAIM) were investigated with Polypropylene (PP) and Stainless Steel Powder Feedstock (SSPF). The selected processing variables were melt temperature, shot size, gas pressure, and gas delay time. By using a Taguchi L_9 array, the results were compared with previous work. For PP, there were no significant differences on gas penetration depth. However, the significance of gas delay time was relatively higher in an Al cavity as compared to a Stereolithography (SLA) cavity from previous work with SSPF. The most significant parameter affecting RWT was melt temperature for PP and gas delay time for SSPF, respectively. Additionally for SSPF, we found that gas penetration depth and RWT decreased with increasing mold temperature.

DEDICATION

This thesis is dedicated to my wonderful family. My mother, my father, and my younger brother wholeheartedly inspired, motivated and supported me all the way. Thank you for your unconditional love and support that you have always given me. Thank you for everything. I love you.

ACKNOWLEDGMENTS

I will always be grateful to Dr. Kye Hwan Lee, Chair of my thesis committee, for all his mentoring and advice. The completion of my master's course would not have been possible without his infinite patience and guidance. My thanks go to my thesis committee members: Dr. Seokyoung Ahn, Dr. Rajiv Nambiar, Dr. Miguel A. Gonzalez, and Dr. Douglas H. Timmer. Their advice, input, and comments on my thesis helped to ensure the quality of my intellectual work.

I would also like to thank Hector Arteaga and Rene Maldonado for their guidance and technical support. I am always grateful to Dr. Bong Lee and Dr. Joo Hyun Kim who gave me the opportunity to study in USA and the interest in study. Also, I would like to acknowledge everyone who helped me in various ways.

TABLE OF CONTENTS

LIST OF TABLES

Page

LIST OF FIGURES

Page

CHAPTER I

INTRODUCTION

Injection molding technology has become one of the most popular manufacturing processes due to its capability to efficiently produce precision plastic components with the possibility of processing wide ranges of materials. The cycle time is also significantly less compared to the other manufacturing techniques.

As with the material flexibility of injection molding, Powder Injection Molding (PIM) has particularly presented an effective and mature technology which is able to produce complex shaped products through injecting metal or ceramic in substitute for plastic materials into the cavity [1]. The PIM allows the fast cycle time and low cost production of small-sized complex metallic components with high dimensional accuracy consistently. It is considered as a more superior technology than general powder metallurgy or precision casting [2, 3].

However, the powder used in PIM is very minute as around 10μm and is two times or more expensive than the powder used in general powder metallurgy (about 150μm). More content of binder (35~60 Vol.%) is also necessary to maintain the proper fluidity required in the PIM process compared to the other powder molding technologies. Consequently, the contraction rate of parts is high (above 10%) after sintering, and de-binding takes a long time from 24 to 120 hours. Due to the minute particle diameter of powder, the weight per unit volume of sintered parts is greater in PIM than in the other

sintering methods, and the heavy weight is very disadvantageous in the cost of the product [1].

Gas-Assisted Injection Molding (GAIM) is a modification of the conventional injection molding and a method of pressurizing an injection molding part with gas in order to provide the necessary packing force to produce a quality injection molded part [4]. The GAIM has many advantages when it is compared to the conventional injection molding processes. GAIM produces parts with hollow internal sections and this becomes particularly useful for PIM since less law material can be used. Required time for de-binding processes can be reduced as well [5]. Despite the advantages, the GAIM process with powder feedstock, i.e., Gas Assisted Powder Injection Molding (GAPIM) process is not intensively studied. Also the effect of processing variables over GAPIM process is not well understood yet.

According to the previous researches [6-8], it was recognized that GAIM has a capability and applicability to the PIM process. Epoxy cavities made by Stereolithography (SLA) were used in the prior experiments by Lee et al. [8] due to simple fabrication and low cost. The durability of SLA cavities was significantly increased by the application of GAPIM due to reduced injection pressure in the experiments [9]. However, use of metal cavities is necessary in order to accomplish mass production and commercialization. Accordingly, this research will focus on the effects of the processing parameters such as melt temperature, shot size, gas pressure, and gas delay time on gas penetration depth using an Aluminum (Al) cavity insert. Simulations and experiments were conducted to find the effects of processing variables and the results were compared to the previous experiment using a SLA cavity. Furthermore, Residual

Wall Thickness (RWT), which is also important for commercial application of GAPIM, was investigated. The effect of differential mold temperature on gas penetration and RWT was also performed.

CHAPTER II

REVIEW OF LITERATURE

Powder Injection Molding Process

PIM is one of the powder molding techniques which produces metal or ceramic components. It has been applied to ceramics for several decades, but it began to be widely commercialized in the 1980s with major progress in forming ceramic heat engine components with the technology. Subsequently, it has been practiced extensively to fabricate near-net-shape parts for a wide variety of industries [1]. PIM has been successfully applied into the industries associated with several automotive, medical and consumer electronics applications. Worldwide PIM sales already exceeded the $1 billion mark and the sales for metal injection molded components reached about $800 million in 2007 [10]. Figure 1 shows the breakdown of the worldwide sales based on the previous synthetic data.

PIM technology includes four successive processes and they are mixing, injection molding, de-binding and sintering [3]. Figure 2 shows the schematic of the process. After metal or ceramic powder is blended with binder made by organic materials, the parts are molded with the prepared feedstock using a typical plastic injection molding machine. Two processes such as de-binding to remove the binder from the parts and then sintering to densify the parts are followed to obtain the final metal or ceramic products [11]. All steps in the process can affect the mechanical properties of the sintered parts

[11-13]. Accordingly, PIM, which is a combination of powder metallurgy and conventional injection molding, has the capabilities to produce small-sized complex components in great quantities and at a low price, while these capabilities are not able to be accomplished by the other powder metallurgy processes due to the flow limitation of powder and the difficult transmission of compressive force. [1]

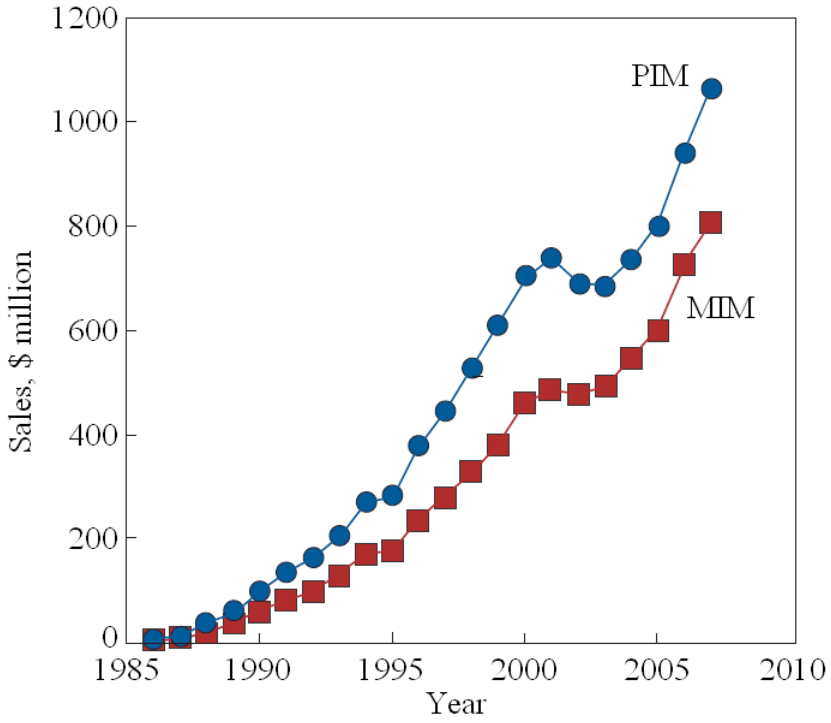

Figure 1. Worldwide annual sales for PIM and MIM [11].

PIM can be classified into Metal Injection Molding (MIM) and Ceramic Injection Molding (CIM) depending on the type of powder used for feedstock. MIM has been a widely used process. The differences between conventional injection molding and MIM are due to the faster cooling and solidification of metal than plastic. The internal defects such as bubbles and cracks or the external defects such as weld lines may occur in parts during molding. Also the elasticity and strength of the molded parts are extremely

low and often causes green part failure. Furthermore, due to the addition of binder to the powder, the parts shrink during the molding process, and the volumetric shrinkage occurs with the amount of removed binder during the sintering process [14].

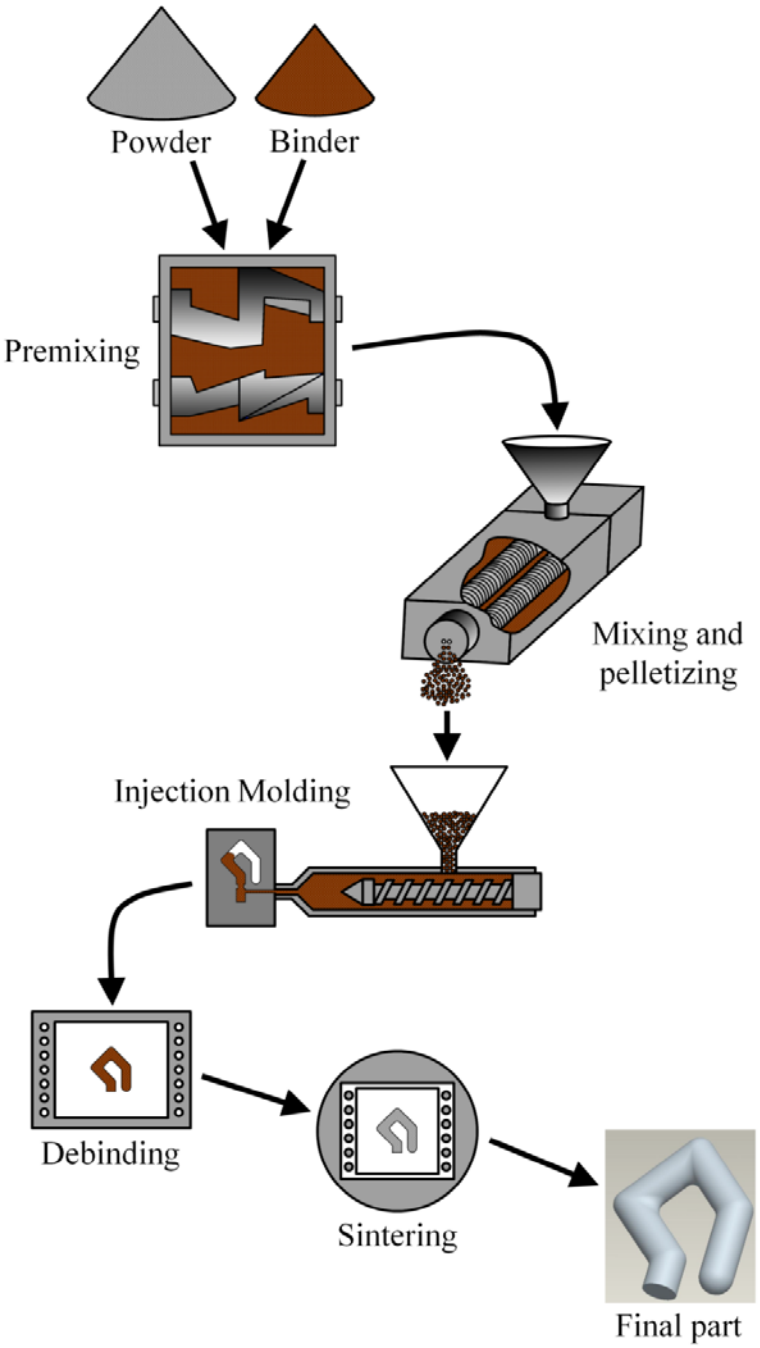

Figure 2. Schematic diagram of PIM process [1].

The advantages of PIM can be identified by five features: low production costs, shape complexity, tight tolerances, applicability to several materials, and superior final properties [1]. MIM is very economical for small complex geometries. Due to excellent dimensional tolerance, it is controllable within the range of 0.3%, and smaller components allow more precise control of dimensions [15]. Accordingly, MIM is usually applied to the fabrication of small-sized complex components of high value with various materials [12, 16, 17]. Based on MIM technology, researches and developments to manufacture micro-structured components are also active which can be applied to various industries [18]. Additionally, since the use of fine powder feedstock promotes the densification of the parts during the sintering process, high quality parts, which have good surface finish and are difficult to be sintered by conventional processes, can be produced [1]. Small powder with diameter generally less than 20μm is used in the MIM process in order to increase sintering density. However, small size powder increases part cost. The metal powder feedstock has lower fluidity than polymer materials, and de-binding for large components requires many hours because the time for binder removal depends on the section thickness. The goal in de-binding is to remove binder from the parts in the shortest time with the least impact on the compact [1, 15].

Karatas et al. [17] recently studied the mouldability of various feedstocks used in PIM. He mentioned that since the feedstocks used in PIM had higher thermal conductivity which leads to fast solidification, very high injection rates were required. The high rates induce the accumulation and separation of binder in sudden direction changes in the cavity during injection molding. This separation caused the defects in the sample during de-binding and sintering. In his experiment, the moldability increased with

increasing injection parameters such as pressure, temperature, and flow rate and with the low viscosity of feedstocks.

PIMSolver (Cetatech, South Korea), which is one of the Computer Aided Engineering (CAE) analysis software for the PIM process, is not only capable for part design and mold design, but also the optimization of processing conditions for injection molding machine during the design stage, so that cost and time for development can be saved [18]. Urval et al. [19] recently achieved the quantization of the influence of decreasing part thickness with accompanying increase in aspect ratios on the process parameters, including melt temperature, mold temperature, fill time and switchover position, using the Taguchi method experiment and PIMSolver. He mentioned that as the part thickness reduced, higher melt temperature and mold temperature would be necessary to obtain complete parts due to the faster solidification. The mold temperature was the most critical parameter.

Gas-Assisted Injection Molding Process

GAIM technology has been increasingly adopted due to many advantages over conventional injection molding. Injection-packing pressure, cooling time, and material use can be reduced. Injected parts has more uniform properties such as reduced sink mark, shrinkage, warpage, and residual stresses, resulting in better final production at lower costs [20-23]. GAIM is a technology which injects gas to form hollow cores in the thicker sections of the part [24]. Figure 3 shows the process of GAIM in four stages.

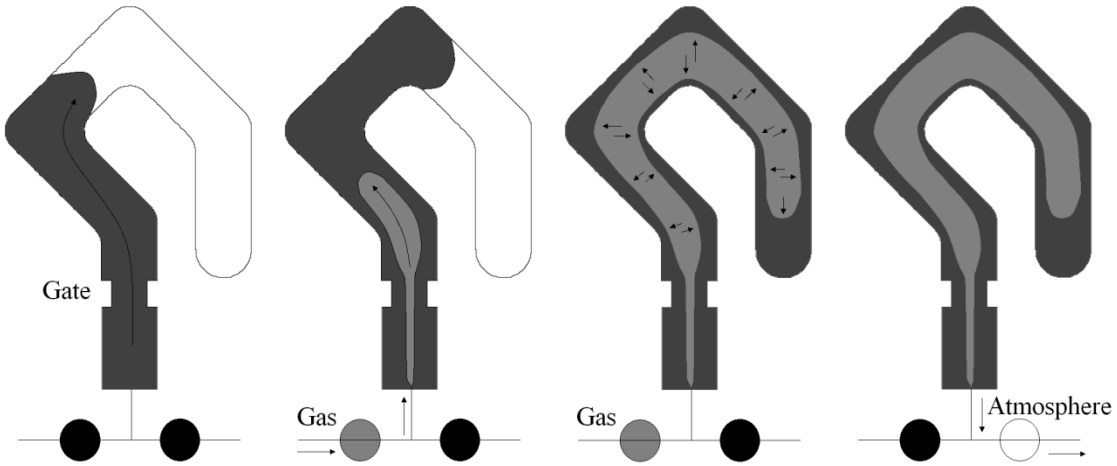

Figure 3. Schematic diagram of GAIM.

In the first stage, a fixed amount of plastic melt is injected into the mold cavity which is called as “short shot” (less than the full volume of the cavity). The injection pressure required is reduced due to less filling in the cavity as compared to conventional injection molding. In the second stage, the nitrogen gas is injected and the plastic melt is displaced by applied gas pressure. It takes the path of least resistance ideally along the center section of thicker channels that are at a relatively high temperature. In the third stage, the gas pushes the plastic melt from the thick section of the part to the unfilled extremities of the vented cavities, thereby filling the part and leaving a hollow section in the channel. The gas continues to apply pressure as the plastic cools, solidifies, and packs more efficiently. The pressure that is applied against the walls of the mold cavity is lower than the packing pressure used in conventional molding. Further, the gas is compressible and so applies a uniform pressure on the inside surface throughout the part. This results in better packing, thus minimizing sink marks and surface blemishes which lead to a more aesthetically pleasing part [4, 25]. In the fourth stage, the part is completely cooled and the gas is vented before the mold opens.

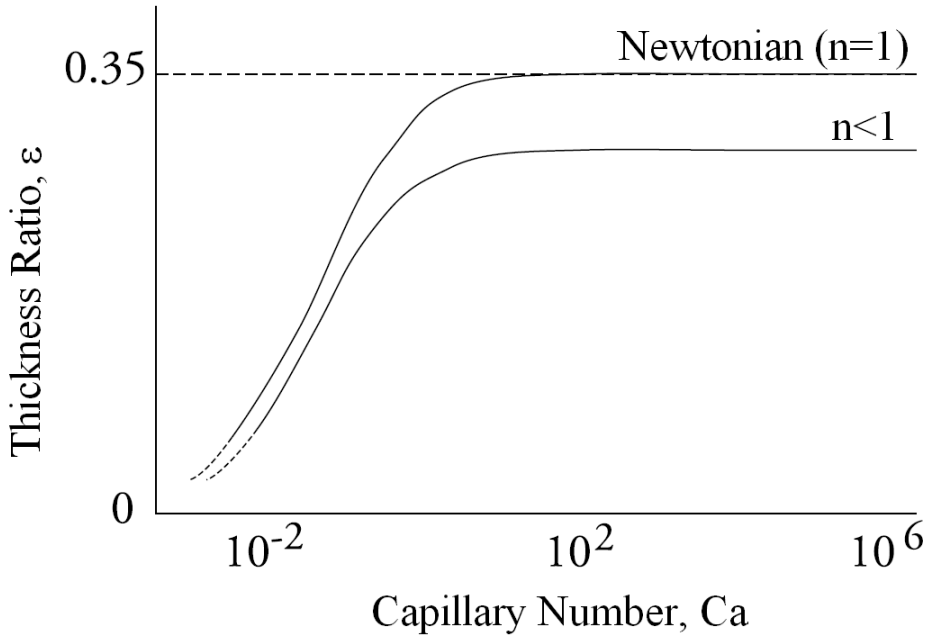

Figure 4. Thickness ratio versus Capillary number [21, 22].

Poslinski et al. [26] investigated gas assisted displacement of viscoplastic liquids in tubes. He found that RWT could be determined by Capillary number (Ca) which shows asymptotic behavior.

$$\mathrm{Ca} = \frac{\mu U}{\gamma} \tag{1}$$

where μ, U, and γ are the viscosity, gas penetration rate, and surface tension of the liquid. Figure 4 shows the effect of Ca on the thickness ratio ε

$$\varepsilon = \frac{\delta}{R} \tag{2}$$

where δ is the RWT and R is the radius of the tube. He also concluded that RWT was determined by the gas penetration rate. When the gas penetration rate was low, the more liquid of material was displaced from the molten layer to the front of the gas core

inducing the thinner frozen layer and the RWT increased linearly from the gas injection point to the blowout location. On the other hand, when the gas penetration rate was high, the thickness distributed uniformly and the thickness ratio approached $\varepsilon = 0.35$. He mentioned that the gas front moved faster than the liquid front and it accelerated due to the decrease in the amount of the liquid front corresponding to the displacement to the melt layer.

Chen et al. [27] studied the characteristics of gas penetration in a spiral tube and he found that the RWT behind the gas front was uniformly distributed in the primary gas penetration stage. On the other hand, two types of characteristics on RWT were observed near the gas front. In the parameter setting levels of low gas pressure and high gas delay time, the RWT decreased first and then increased significantly due to the secondary gas penetration which occurred by the shrinkage of solidifying plastic. In the level of high gas pressure and low gas delay time, the RWT increased dramatically.

Yang et al. [28] studied the uniformity of RWT distribution around dimensional transition and curved sections in circular tubes, since the RWT was not uniform near transitions. The uniformity of RWT in the transition was improved by the addition of fillets. He also mentioned that the inner wall thickness is always thinner than the outer wall thickness in curved sections due to the different distance between gas front and melt front. The difference was decreased with low melt temperature, high mold temperature, and high gas delay time.

Recently, there was an experiment to improve the RWT uniformity around curved sections in a tube by varying mold temperature [29]. According to this experiment, the RWT uniformity could be improved by the differential mold temperature. Since a

higher mold temperature caused a lower viscosity of the polymer melt, gas penetrated more at outer side of the tube in the curved section.

Gas-Assisted Powder Injection Molding Process

GAPIM is a combination of GAIM and PIM which provides the advantages of GAIM for the PIM process as identified in Figure 5.

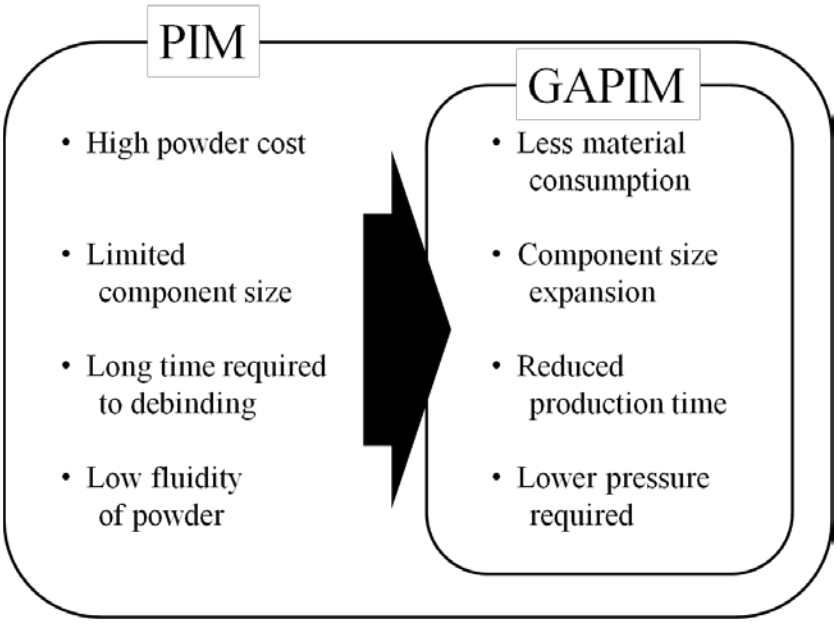

Figure 5. Advantages provided by application of GAIM to PIM.

While the PIM process has a high economical efficiency in the manufacturing of small components, the economical efficiency decreases as the component size increases. As mentioned above, it is due to the expensive powder cost and long de-binding time to remove the binder. However, with the application of GAIM technology to PIM process, the cost of production can be lowered and the time for de-binding can be also reduced. Additionally, a high aspect ratio and superior molding quality can be obtained by providing enough gas pressure during injection molding of metal powder feedstock

which will lower fluidity compared to polymer materials. Qingfa [6] mentioned that the lower material consumption and the ability to apply the technology to large components with thick wall sections are great advantages of GAPIM. According to his technical report, the injected parts were successfully sintered.

Michaeli et al. [7] also performed a GAPIM experiment using a curved spiral tube geometry cavity and Al_2O_3 ceramic powder feedstock. The thermal conductivity of the material was about five times greater than unfilled polypropylene, which implied the availability of shorter gas delay times due to the faster solidification of the feedstock during the mold filling stage of the injection molding cycle. He focused on the wall thickness and its distribution along the melt-flow path in order to investigate the influence of the processing conditions, including gas pressure, gas holding time, shot size, and gas delay time. Among the parameters, the gas delay time was the most significant factor for the wall thickness, and the wall thickness increased according to the increase of gas delay time. Furthermore, the melt temperature and mold temperature were considered influencing the mass of the part. The lower mold temperature was accompanied with the greater mass of the part. When the difference between the melt temperature and mold temperature was high, the feedstock froze fast with a thick frozen layer. On the other hand, when the difference between the temperatures was low, the feedstock froze slowly and the gas bubble pushed more melt into the cavity, resulting in decreased wall thickness and lower mass of the part. There were less significant effects of other parameters on the wall thickness.

Recently, Lee et al. [8] studied the effects of the processing parameters such as melt temperature, shot size, gas pressure, and gas delay time on the gas penetration depth

and RWT in the GAPIM experiment in which a SLA cavity was introduced. The Taguchi L_9 array based on Design of Experiments (DOE) was used in simulation runs with the AMI software (Autodesk Moldflow Insight, USA), and experiments for GAIM with PP and for GAPIM with SSPF were run. Despite the simulation prediction that the shot size was the only significant parameter on the gas penetration depth in GAIM and GAPIM, the experimental results based on the significant effects of the processing parameters deviated from the simulation result. He found that the shot size and gas delay time were equally significant parameters in the GAIM experiment and the shot size, gas pressure, melt temperature were equally significant parameters in GAPIM experiment. He also mentioned that the difference between the simulation and the experiment was due to the insensitivity of the simulations ability to associate the gas pressure, gas delay time, and melt temperature. Additionally, the effects of the processing parameters on RWT were insignificant in the GAPIM experiment using the SLA cavity, and it indicated that the RWT was not in control with the SLA cavity.

CHAPTER III

METHODOLOGY

Processing Materials

Polypropylene (PP) random copolymer, 13T10Acs279 from Flint Hills Resources (Odessa, TX), was used in the GAIM experiment. The PP is one of the most widely used crystalline polymers in injection molding process. The crystalline polymers tend to have higher shrinkage rate than amorphous polymers [30]. The PP has excellent impact resistance, flexural modulus, and clarity which allows the easy observation of gas penetration. It is commercially applied for the wide ranges of products from lab ware and food packaging to automotive applications. The material selected for the GAPIM experiment was stainless steel powder SUS316L (Cetatech, South Korea) combined with a wax-polypropylene based binder and a powder loading of 59Vol.%. Various medical parts and cellular phone parts are produced with the Stainless Steel Powder Feedstock (SSPF). Table 1 shows the properties of PP and SSPF used in this research. The simulation runs were also conducted based on the input data. Due to the higher thermal diffusivity of the SSPF than PP, a more rapid and uniform change of temperature is induced in the solid layer in the cavity. Additional properties of the materials are exhibited in Appendix A, and the information was also used to perform AMI simulation which is described in this chapter.

Table 1. Material properties.

Property	**PP**	**SSPF**
Density (g/cm^3)	0.9	7.76
Specific heat capacity (J/Kg-C)	2740	685
Thermal conductivity (W/m-C)	0.16	1.84
Thermal diffusivity (m^2/s)	0.65×10^{-4}	3.46×10^{-4}

Part and Mold Design

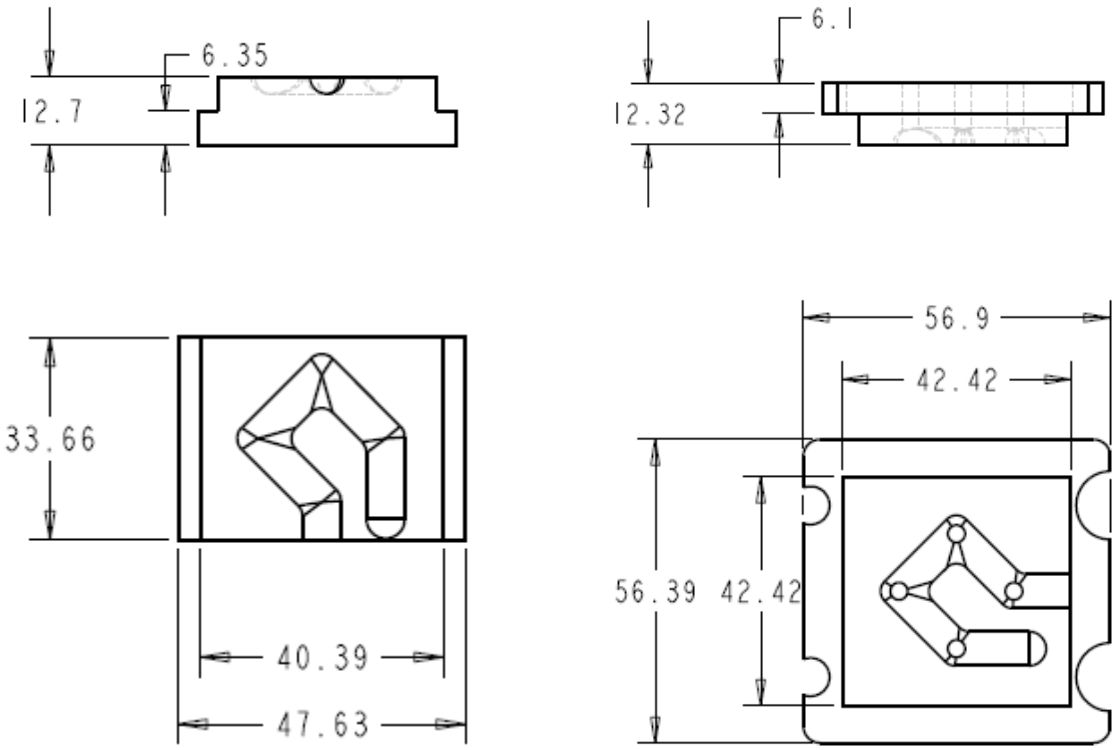

(a) (b)

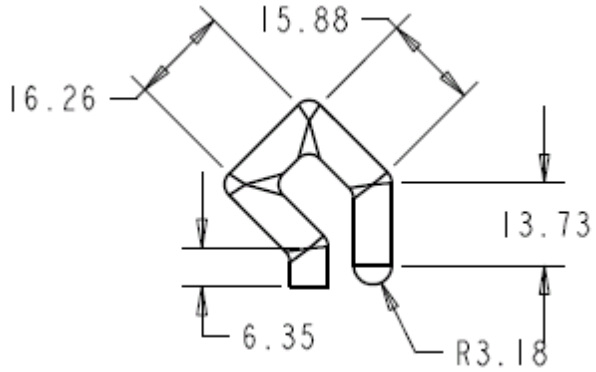

(c)

Figure 6. Dimension for (a) mold cavity inserted in injection mold, (b) mold cavity inserted in ejector mold, and (c) the part. All dimensions are in mm.

The geometry as shown in Figure 6 consists of a hook shaped part with a 6.35 mm diameter cylindrical cross section that has a sequence of angular turns of 45°, 90°, 90° and 45° in order to study the effects of angles on the flow of powder metal in the cavity. The cavities were built by CNC tooling with Al, as shown in Figure 7.

Figure 7. Al cavities.

Processing Equipment

The molds were mounted into a Master Unit Die quick change insert with an 84/90 ALU 210 mold frame. Injection molding was conducted through a 30 ton Boy 30M injection-molding unit as shown in Figure 8. The unit has a maximum stroke of 95 mm with a maximum barrel capacity of 37 grams and a screw diameter of 28 mm. The fixed processing conditions for the experiment are listed in Table 2. More injection pressure was required in this experiment compared to Lee's [8] using the SLA cavity due to the faster cooling on the surface of the metal cavity than a SLA cavity. The faster cooling caused lower flow of the feedstock into the cavity.

Figure 8. Boy 30M injection molding unit.

Table 2. Fixed processing conditions.

Parameter	Value
Injection Pressure	8.48 MPa
Hold Pressure	6.89 MPa
Back Pressure	0.52 MPa
Clamping Force	11.0 MPa
Screw Speed	50.0 rpm

Figure 9. Gain Technologies nitrogen generator.

Figure 10. Gas pressure regulation control unit.

A nitrogen supply for GAIM was obtained through a nitrogen generator from Gain Technologies (GT-N2GA). Membrane separation technology separates compressed air into streams of 99.5% nitrogen and mixed oxygen with carbon dioxide traces. A gas control system from HEA International was used.

A K-Type Omega TT-J-30-SLE thermocouple was placed 2 mm below the surface of the part cavity used to measure the mold temperature. Real time data from the mold was recorded using a National Instruments data acquisition board. The temperature monitoring system was calibrated with Omega HH21A temperature meter with 0.5°C resolution. Mold temperature was maintained at 30°C during the DOE. However, after optimum processing conditions were found, mold temperatures were varied from 30°C to 60°C in order to study the effect of mold temperature over RWT. The mold temperature was monitored by the installed thermocouple and the cooling time was set to maintain constant mold temperature from shot to shot.

Design of Experiments

In the injection molding process, there are many parameters that have an effect on the properties of the injected parts. Particularly, in the GAIM process, additional parameters associated with the gas control such as gas pressure, gas delay time, and gas inject time have to be considered since the parameters also have a significant effect on the properties of the injected parts. Accordingly, it is necessary to introduce one of the DOE methods such as partial, full factorial design, or Taguchi approach in order to reduce cost and time for the production. The Taguchi method, which is called the “robust design method”, has been widely used in industry and research.

The processing parameters under investigation were: melt temperature, shot size, gas pressure, and gas delay time, as these were known to be the most significant parameters for GAIM [20, 31, 32]. The processing windows were determined after preliminary molding experiments. Low, medium, and high values that were chosen within the processing windows are shown in Table 3. All processing variables used were the same as previous experiments [8] except injection pressure. Due to changes in mold temperature, the increase in injection pressure was necessary in order to maintain constant shot sizes at various mold temperatures. Process parameter variations were done through a DOE approach in order to reduce the number of experiments while maintaining reliability. In this study a 3^4 factor L_9 orthogonal array, which is called the Taguchi method, was adopted as shown in Table 3. From the results of the molding window study the values of the three levels of the processing parameters of the L_9 orthogonal array for both GAIM with PP and GAPIM with SSPF were chosen as shown in Table 4. This processing window has been used for the nine simulation runs and experiments.

Table 3. DOE 3^4 factor L_9 orthogonal array.

Trial	Melt temperature	Shot size	Gas pressure	Gas delay
1	1 (Low)	1 (Low)	1 (Low)	1(Low)
2	1 (Low)	2 (Medium)	2 (Medium)	2(Medium)
3	1 (Low)	3 (High)	3 (High)	3(High)
4	2 (Medium)	1 (Low)	2 (Medium)	3(High)
5	2 (Medium)	2 (Medium)	3 (High)	1(Low)
6	2 (Medium)	3 (High)	1 (Low)	2(Medium)
7	3 (High)	1 (Low)	3 (High)	2(Medium)
8	3 (High)	2 (Medium)	1 (Low)	3(High)
9	3 (High)	3 (High)	2 (Medium)	1(Low)

Table 4. Molding window for PP and SSPF.

Process	Level	Melt temperature	Shot size	Gas pressure	Gas delay
PP	**1**	193 °C	73%	5.65 MPa	0.5 s
	2	204 °C	76%	5.79 MPa	1.0 s
	3	216 °C	79%	5.93 MPa	1.5 s
SSPF	**1**	150 °C	69%	6.21 MPa	0.0 s
	2	155 °C	72%	6.55 MPa	0.2 s
	3	160 °C	75%	6.89 MPa	0.4 s

In this study, our target function is to obtain maximum gas penetration depth and RWT. The statistic Signal to Noise ratio (S/N ratio) is the ratio of the power of the signal

to the power of the noise. The larger-the-better S/N ratio calculation shown below was used to achieve maximum gas permeation and RWT:

$$S/N = -10\log\frac{1}{n}\sum\frac{1}{y_i^2} \quad (3)$$

where n is the number of data points and y_i is the measured data. The S/N ratio is used to identify the parameter values for the optimal result.

Simulation of Gas-Assist Injection Molding

According to a recent paper [13], commercial software for the simulation of thermoplastic injection molding can be usefully applied to MIM simulations, since the thermoplastic and metal feedstock have similar material properties. The AMI software was employed to understand the effects of processing parameters on gas penetration depth and RWT through simulation runs. The gas penetration depth and RWT were obtained through the measurement tool in the AMI software, and were compared to the values obtained from the experiment. The material properties of PP used in this experiment were readily available in the AMI materials database. The viscosity and pressure-volume-temperature (*pvT*) data for SSPF were imported from the database file provided by Cetatech.

Simulation Procedures

The properties of Al which were the materials of the mold and cavity were used from the AMI material database. The processing parameters used are listed in Table 4. The gas penetration depth and RWT were measured for each simulation result using the measurement tool in the AMI software. From the results of the gas penetration and RWT, S/N ratio analysis were conducted to find the effects of the processing parameters on the

gas penetration depth and RWT and to obtain the optimum processing parameter levels. Based on the optimum processing conditions obtained for the gas penetration depth in the GAPIM simulation with SSPF, additional simulation runs were conducted to investigate the effect of mold temperature on gas penetration depth and RWT. The mold temperature was varied from 30°C to 60°C, according to the recommended range of mold temperature for SSPF.

Experimental Procedures

A cooling time of one minute was incorporated between every injection cycle in order to maintain a constant temperature for the cavity surface and mold. The experiment trials were randomized to minimize the noise. After the process was stabilized, the first five samples were discarded, and then ten good samples were collected from each trial. Five samples were used to measure the gas penetration depth and the other five samples were used to measure the RWT. The five molded parts for gas penetration depth measurements were cut in halves along parting lines to make the gas penetration visible, and the other five parts for the RWT measurements were also cut in four locations. Measurements were taken with a Vernier caliper. The measured gas penetration depth and RWT were then used to conduct the analysis based on a DOE orthogonal array. S/N ratio analyses were conducted to find the effects of the processing parameters on the gas penetration depth and RWT, and to obtain the optimum processing parameter levels. Based on the optimum processing conditions obtained for the gas penetration depth, additional experimental trials were conducted to investigate the effect of mold temperature over gas penetration depth and RWT.

CHAPTER IV

RESULTS AND DISCUSSION

As explained earlier, an Al cavity insert, in place of a SLA cavity used in previous research [8], was introduced throughout simulation runs and experiments. Due to the higher thermal conductivity of the Al cavity insert, the mold temperature control associated with the cooling of injected plastics and powder feedstock was possible. The simulation runs and experiments for GAIM and GAPIM were conducted based on the processing parameter settings from Table 4 in order to find the effects of the processing parameters on gas penetration depth and the optimum processing conditions for the highest gas penetration depth. Then the effect of the processing parameters on RWT was also considered. Additionally, since mold temperature was also significant parameter in previous studies with plastics [33], it was varied in the simulation runs and experiments to explore the effect of mold temperature (or cooling effect) on the gas penetration depth and RWT after the optimum processing conditions were obtained. It will be discussed later in this chapter.

Effects of Processing Parameters on Gas Penetration

Simulation Results

The gas penetration depth for each of nine trials was obtained through the measurement of each gas bubble using the measurement tool in the software. Figure 11 and 12 show the gas penetration depth in the simulation runs for GAIM and GAPIM,

respectively. In both cases, trial 1, 4 and 7, which were applied with the lowest setting level for shot size, have the highest relative penetration depth, indicating that the lower shot size settings yield higher gas penetration depth.

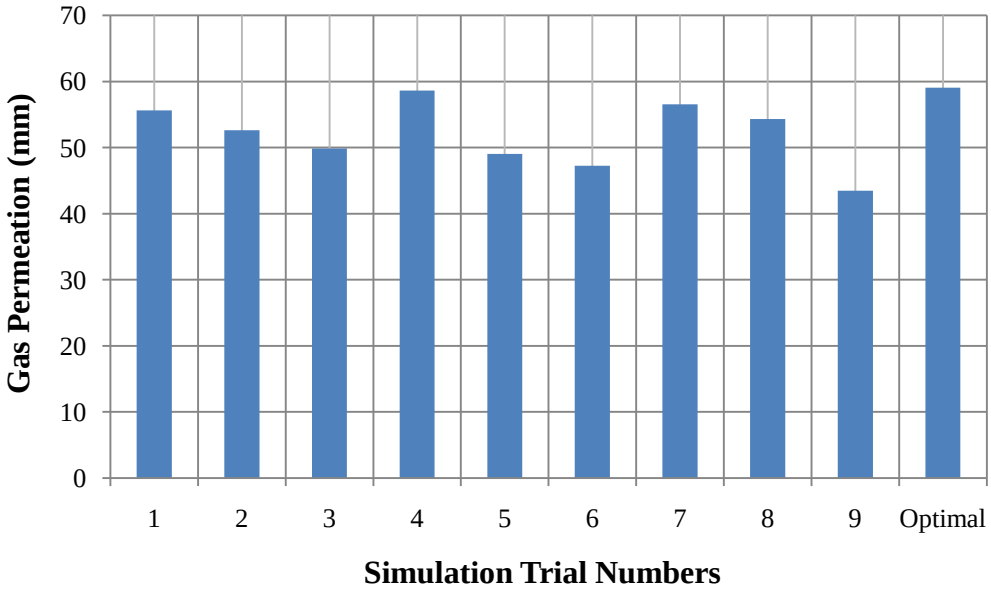

Figure 11. Gas penetration depth for simulation of GAIM with PP.

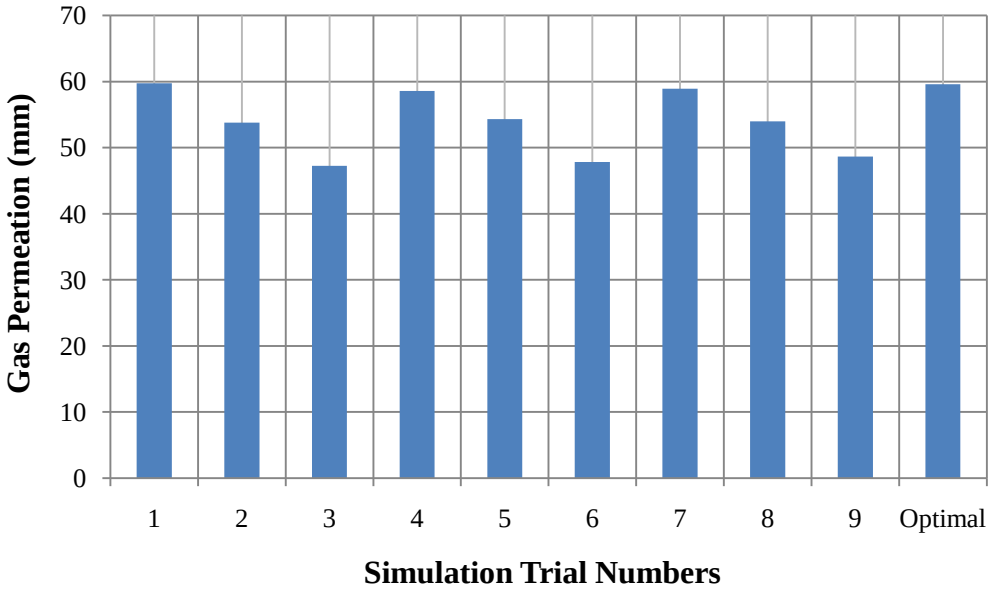

Figure 12. Gas penetration depth for simulation of GAPIM with SSPF.

S/N ratios were calculated from the values of the gas penetration depth corresponding to Figure 11 and 12, and those were used to get the average S/N ratios for three levels of low, medium, and, high parameter settings. Delta, which is a difference between the maximum and minimum values of average S/N ratios, portions and parameter ranks were then calculated and shown in Table 5 and 6. The significance of the effect on gas penetration depth was identified by the ranked portions. Accordingly, the shot size was the most significant parameter with a portion of 57% in GAIM and with a portion of 87% in GAPIM. This result is in good agreement with previous studies over plastics [20, 24, 31]. The gas delay time was also a significant parameter with a portion of 28% in GAIM, while the effect of the gas delay time showed much lower significance with a portion of 8% in GAPIM. This difference is mainly due to higher thermal diffusivity of the powder metal feedstock compared to PP. This may be a result of fast cooling of injected SSPF. Further discussion will be followed later in this chapter.

Table 5. Process parameter rank of significance on gas penetration for simulation of GAIM with PP.

Level	Melt temperature	Shot size	Gas pressure	Gas delay
1	**34.43**	**35.11**	**34.36**	33.83
2	34.22	34.31	34.19	34.32
3	34.17	33.4	34.27	**34.67**
Delta	0.26	1.7	0.18	0.84
Portion	9%	57%	6%	28%
Rank	3	1	4	2

Table 6. Process parameter rank of significance on gas penetration for simulation of GAPIM with SSFP.

Level	Melt temperature	Shot size	Gas pressure	Gas delay
1	34.54	**35.43**	**34.59**	**34.66**
2	34.55	34.65	34.57	34.54
3	**34.6**	33.61	34.53	34.5
Delta	0.05	1.82	0.05	0.16
Portion	2%	87%	3%	8%
Rank	4	1	3	2

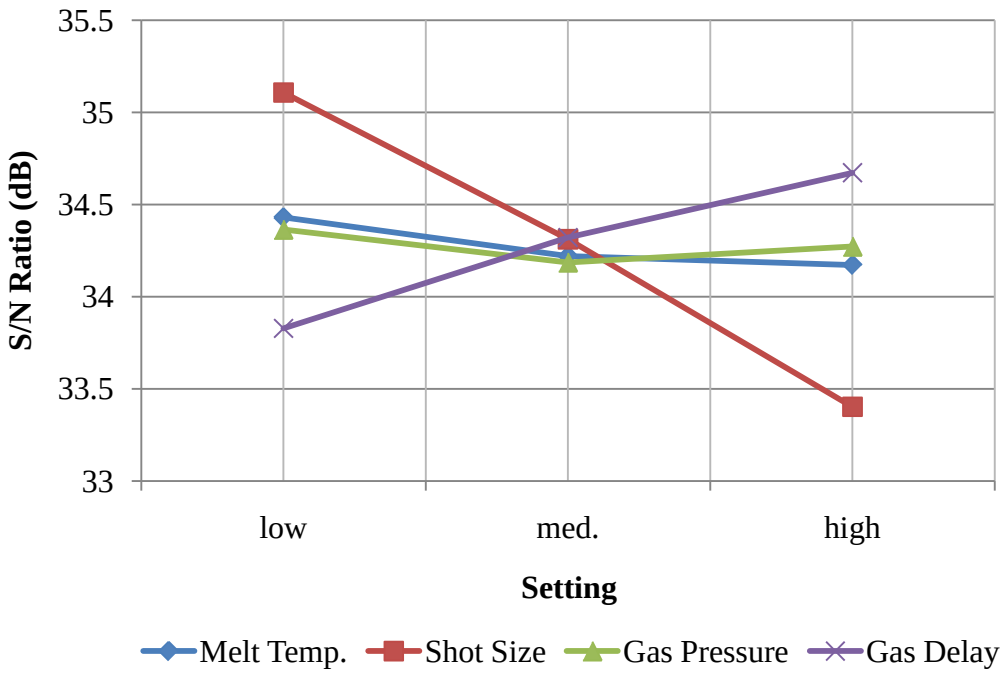

Figure 13. Main effects plots for simulation on gas penetration of GAIM with PP.

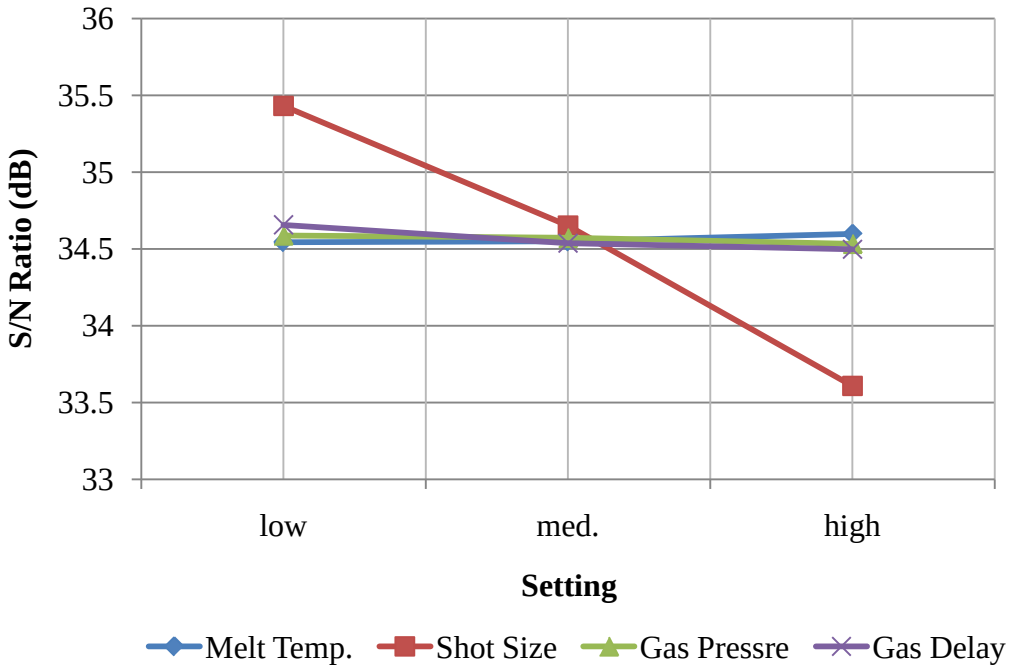

Figure 14. Main effects plots for simulation on gas penetration of GAPIM with SSPF.

Figure 13 and 14 show the main effects plots from Table 5 and 6. Since the target function is to maximize gas penetration depth, the highest S/N ratios in the plots will offer the optimum process setting levels for each of the four processing parameters. From the main effects plots for the simulation shown in Figure 13 the optimum gas penetration depth can be obtained when the melt temperature is low and shot size is low for GAIM. The changes in gas pressure and gas delay time were not significant. For GAPIM shown in Figure 14, the optimum condition for the gas penetration depth was low shot size and other processing parameters were insignificant. There was no difference between the results of the main effects plots using the SLA cavity [8] and the Al cavity in the simulation runs of both GAIM and GAPIM. The gas penetration depth of the parts generated under the optimum conditions in the simulation is also included in Figure 11

and 12, and the part pictures are shown in Figure 15. The shaded regions inside the parts represent the volume of the penetrated gas bubble.

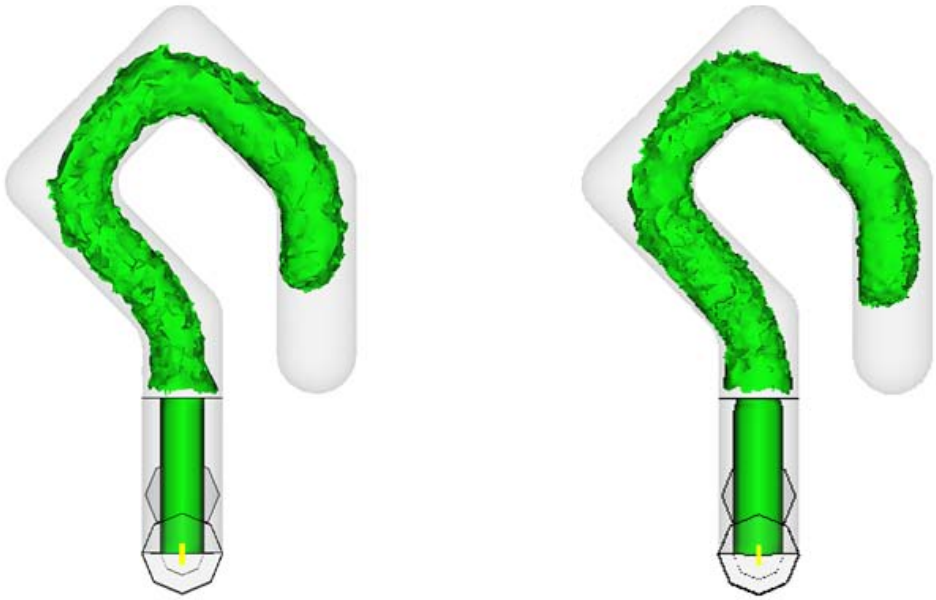

(a) (b)

Figure 15. Gas penetration for AMI simulations of (a) GAIM and (b) GAPIM under optimum conditions.

Experimental Results

The gas penetration depths of molded GAIM PP parts were measured by dying the hollow internal core of the parts with blue ink. However, the gas penetration depths of the GAPIM SSPF parts were measured by cutting the molded GAPIM parts in halves along the parting lines. The averages of the gas penetration depths of five samples in every experimental trial in the L_9 array and the optimum gas penetration depth are indicated in Figure 16 and 17.

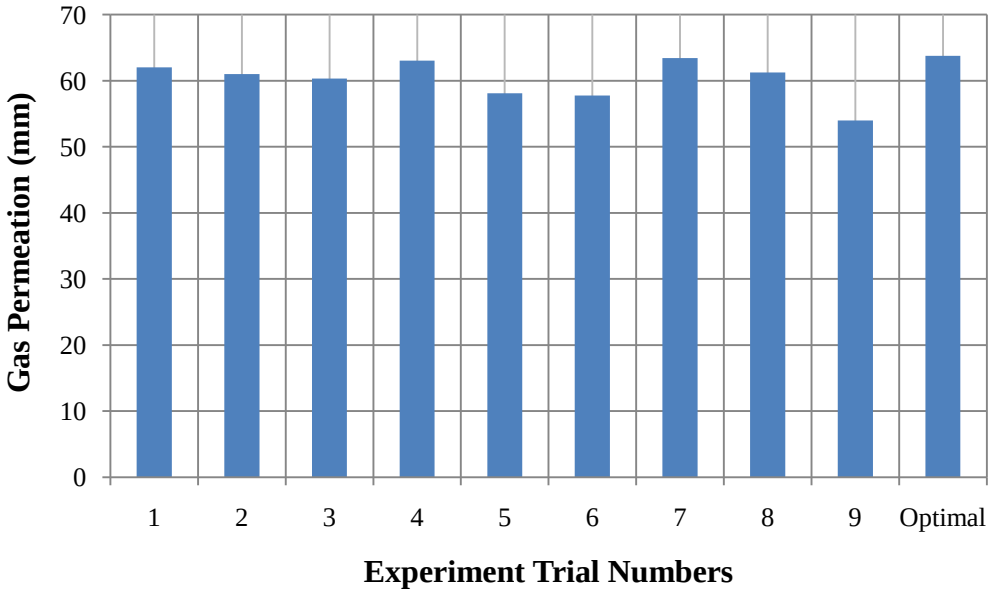

Figure 16. Gas penetration depth for experiment of GAIM with PP.

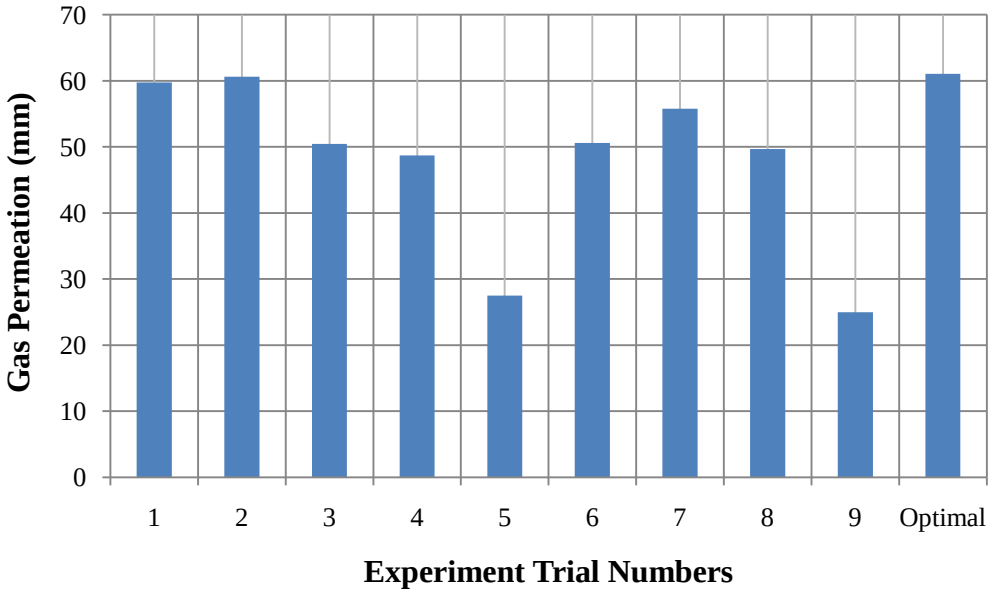

Figure 17. Gas penetration depth for experiment of GAPIM with SSPF.

Table 7. Process parameter rank of significance on gas penetration for the GAIM experiment with PP.

Level	Melt temperature	Shot size	Gas pressure	Gas delay
1	**35.72**	**35.96**	35.61	35.26
2	35.5	35.58	35.45	35.66
3	35.48	35.16	**35.65**	**35.78**
Delta	0.24	0.8	0.2	0.52
Portion	14%	45%	11%	30%
Rank	3	1	4	2

Table 8. Process parameter rank of significance on gas penetration for the GAPIM experiment with SSFP.

Level	Melt temperature	Shot size	Gas pressure	Gas delay
1	**35.08**	**34.74**	**34.51**	30.76
2	32.2	32.78	32.45	**34.89**
3	32.27	32.03	32.59	33.91
Delta	2.87	2.7	2.06	4.13
Portion	24%	23%	17%	35%
Rank	2	3	4	1

The processing parameter ranks of significance calculated from Figure 16 and 17 are presented in Table 7 and 8. Table 7 indicates that shot size is the most significant parameter with a portion of 45% and the gas delay time is also a significant parameter

with a portion of 30% in GAIM. This result does not only conform to the simulation results for PP in this research, but it is also in good agreement with the published research to date [20]. Despite the difference from the result of previous experiments using a SLA cavity by Lee [8] which showed the gas delay time with a portion of 38% and the shot size with a portion of 37%, both parameters of shot size and gas delay time still play a key role in the process of this GAIM experiment using an Al cavity. This result also agrees with previous researches [34, 35]. Moreover, gas pressure is the least significant parameter in both simulation runs and the experiment for PP and agrees with previous experiments and similar research in sensitivity analysis [20, 31]. On the other hand, in the GAPIM experiment using an Al cavity, the gas delay time is the most significant parameter with a portion of 35% and gas pressure is the least significant parameter with a portion of 17%. This result is different from the above simulation results and previous experiments using a SLA cavity which showed that the gas pressure was the most significant parameter with a portion of 33% and the delay time was the least significant parameter with a portion of 13%. The difference implies that the cooling effect is more critical in the GAPIM experiment using an Al cavity than using a SLA cavity. Furthermore, the simulation results showed that the shot size was the most significant parameter and the simulation was not able to predict the effects of the other processing parameters associated with gas control on the gas penetration depth in the GAPIM using SSPF.

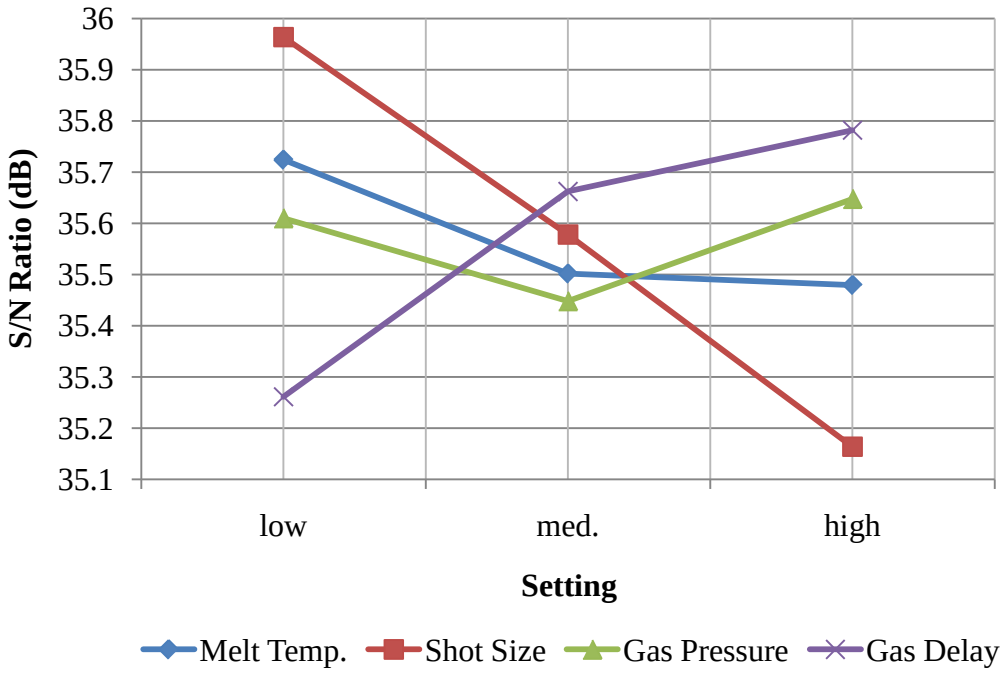

Figure 18. Main effects plots for experiment on gas penetration of GAIM with PP.

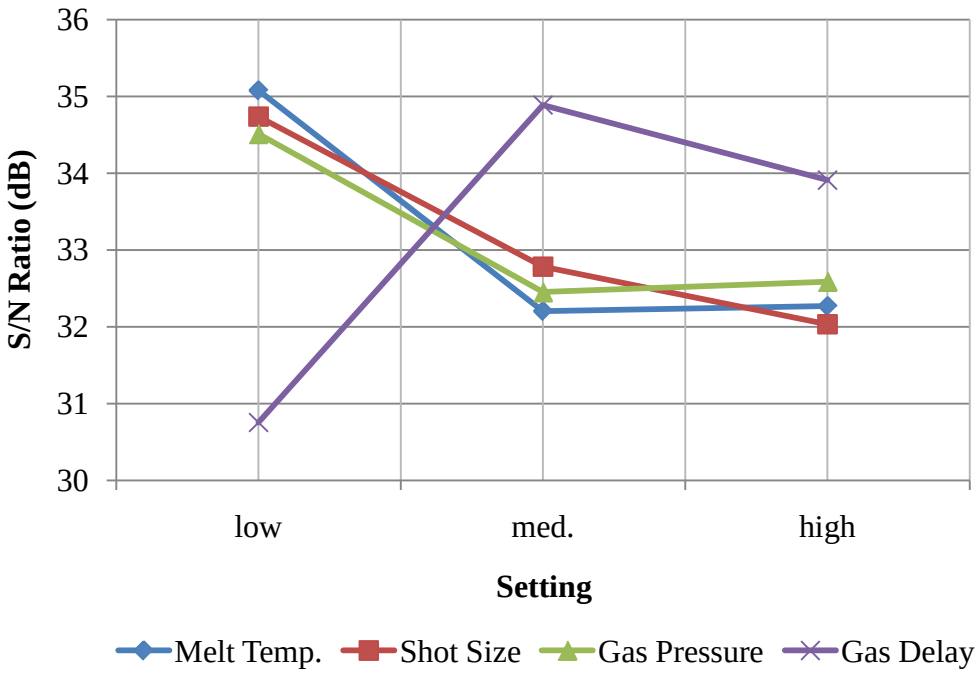

Figure 19. Main effects plots for experiment on gas penetration of GAPIM with SSPF.

The main effects plots in Figure 18 shows that optimum gas penetration depth can be obtained when melt temperature is low, shot size is low, gas pressure is high and gas delay time is high for GAIM. Figure 19 shows that the optimum gas penetration depth for GAPIM can be achieved when melt temperature is low, shot size is low, gas pressure is low and gas delay time is medium.

Figure 20 and 21 show the samples of PP and SSPF parts produced under the optimum parameter setting levels using an Al cavity. The formed internal hollow core of the PP sample was dyed with ink to make it visible.

Figure 20. PP Sample fabricated under the optimum processing conditions showing the gas penetration.

Figure 21. SSPF Sample fabricated under the optimum processing conditions showing the gas penetration.

Effects of Processing Parameters on RWT

Figure 22 shows four RWT measurement locations on the part and a cross section of the locations. RWT at each location was obtained by averaging wall thickness at the four points on the cross section. From the experiment above, the effects of processing parameters on the RWT were analyzed by means of the main effects plots and portion ranks. The target function is to maximize RWT, and the highest S/N ratio in the plot will offer the optimum processing setting levels for each of the four processing parameters. In the simulation and experiment, only section 1 was considered in the analysis because gas penetration depths were not long enough for the RWT measurement in some trials. The other sections will be considered later in this chapter.

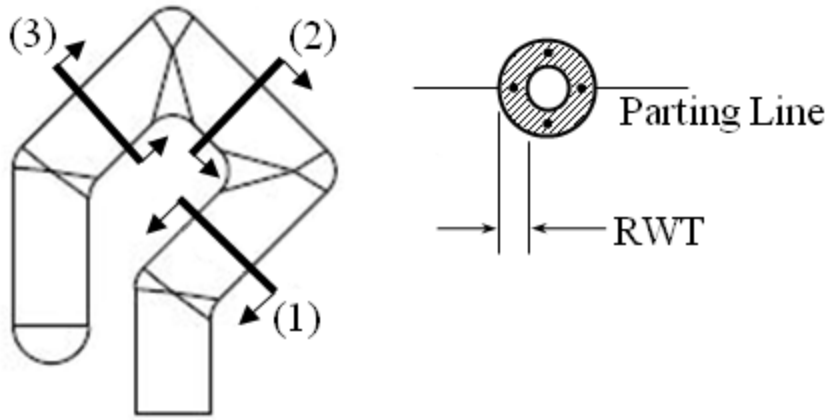

Figure 22. RWT measurement cross sections from (1) to (3).

Simulation Result

The RWT of section 1 for each of nine trials was obtained from simulation runs. Figure 23 shows the RWT for simulations of GAIM and GAPIM, indicating that overall RWT is higher in GAIM than in GAPIM.

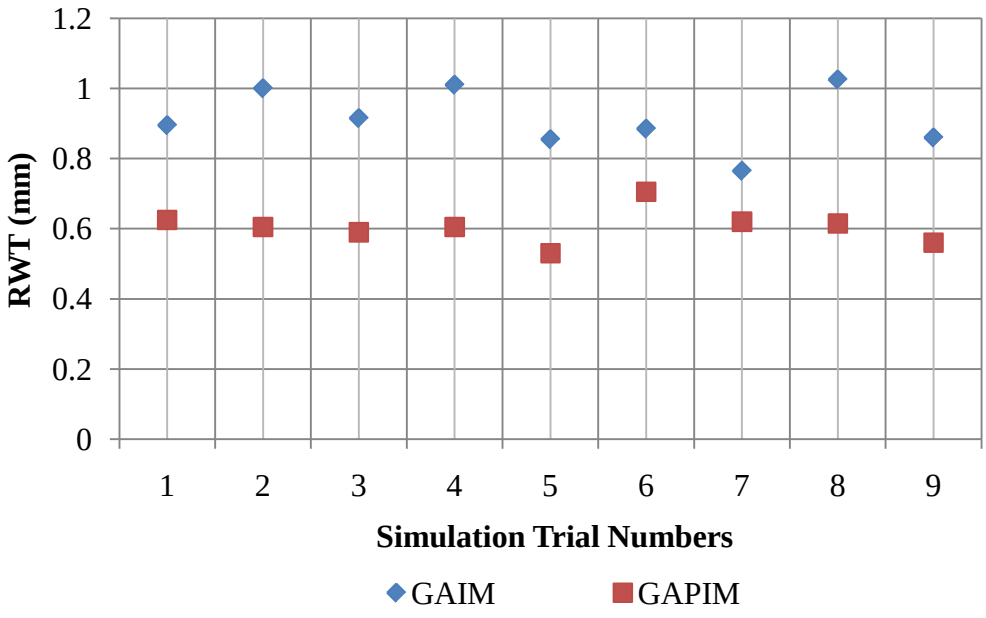

Figure 23. RWT for simulations of GAIM with PP and GAPIM with SSPF.

Table 9. Process parameter rank of significance on RWT for simulation of GAIM with PP.

Level	Melt temperature	Shot size	Gas pressure	Gas delay
1	**-0.58**	-1.07	-0.6	-1.21
2	-0.78	**-0.38**	**-0.41**	-1.13
3	-1.14	-1.05	-1.49	**-0.16**
Delta	0.56	0.69	1.08	1.05
Portion	17%	20%	32%	31%
Rank	4	3	1	2

Table 10. Process parameter rank of significance on RWT for simulation of GAPIM with SSFP.

Level	Melt temperature	Shot size	Gas pressure	Gas delay
1	-4.34	**-4.2**	-3.78	-4.88
2	**-4.31**	-4.7	**-4.59**	**-3.85**
3	-4.47	-4.22	-4.75	-4.39
Delta	0.17	0.5	0.97	1.03
Portion	6%	19%	36%	39%
Rank	4	3	2	1

Table 9 and 10 show the calculated processing parameter ranks of significance on RWT for simulation. Table 9 shows that gas pressure and gas delay time are the most significant parameters with portions of 32% and 31% in GAIM, respectively. Table 10

indicates that gas delay time and gas pressure are the most significant parameters with portion of 39% and 36% in GAPIM, respectively. However, since the values of RWT in simulations were very low, S/N ratios were also very low. With the low S/N ratios, the effects of the parameters on RWT cannot be estimated reliably.

Figure 24 and 25 shows the main effects plots from Table 9 and 10, respectively. For GAIM, low melt temperature, medium shot size, medium gas pressure, and high gas delay time yield the highest RWT. For GAPIM, medium melt temperature, low shot size, low gas pressure, and medium gas delay time results in the highest RWT.

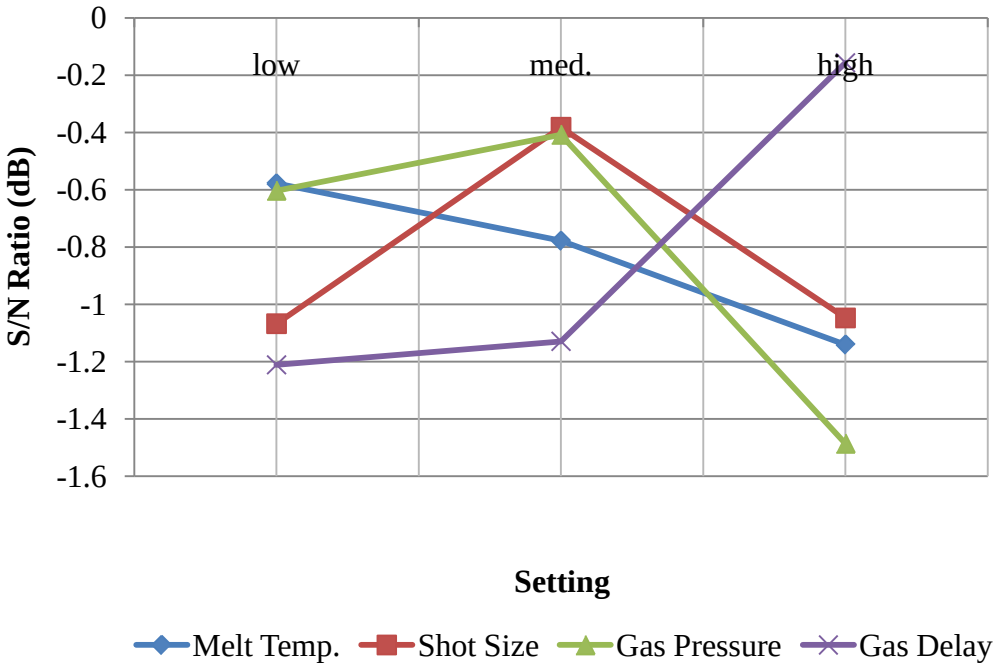

Figure 24. Main effects plots for simulation on RWT of GAIM with PP.

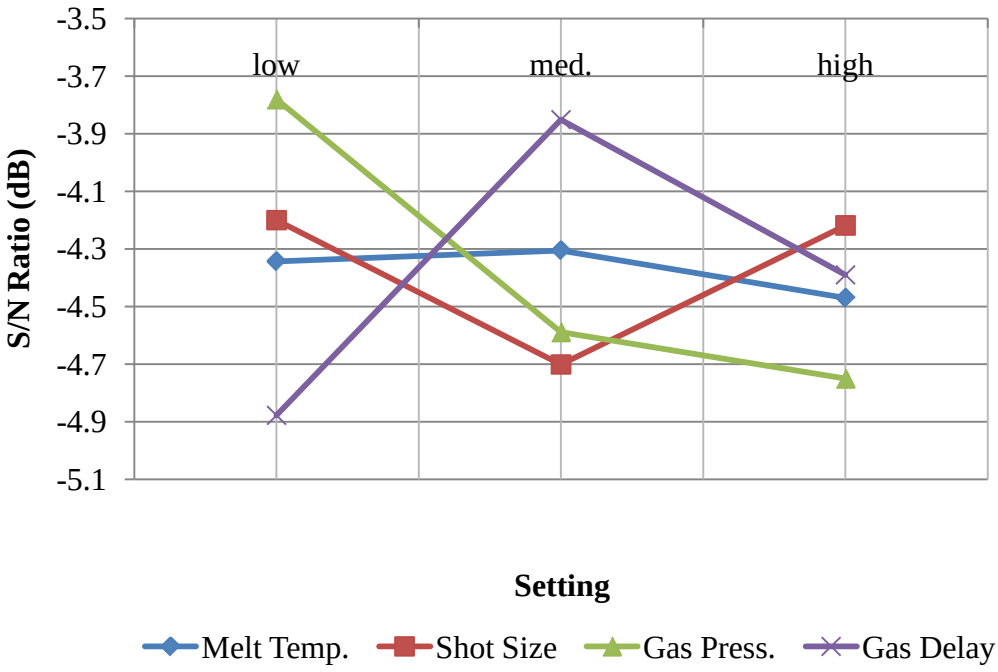

Figure 25. Main effects plots for simulation on RWT of GAPIM with SSPF.

Experiment Result

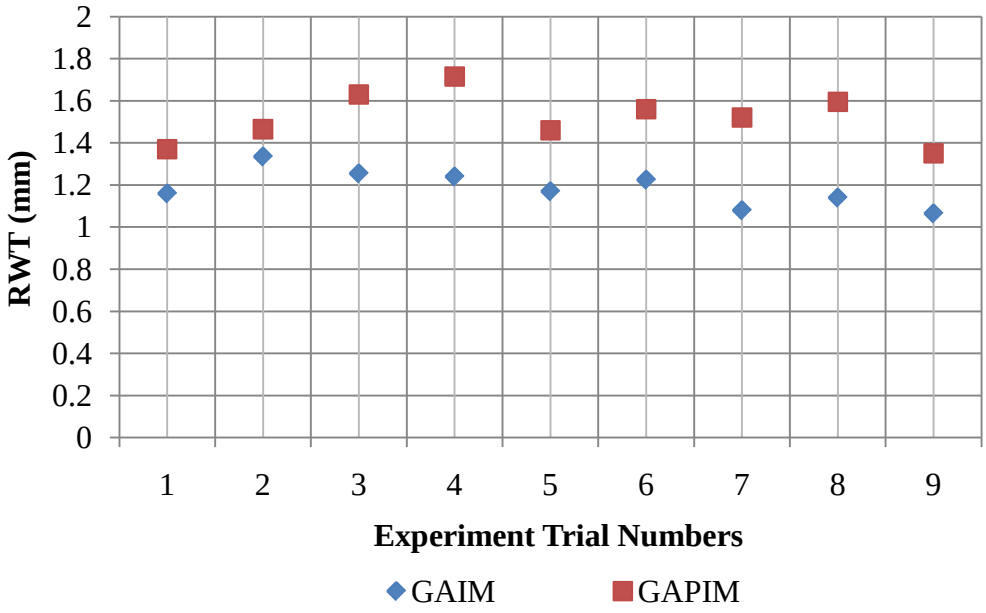

Figure 26. RWT for experiment of GAIM with PP and GAPIM with SSPF.

Figure 26 shows RWT for the GAIM and GAPIM experiment. Overall RWT for GAPIM is higher than for GAIM. This is due to faster cooling of SSPF than PP, resulting in a thicker frozen layer.

Table 11. Process parameter rank of significance on RWT for GAIM experiment with PP.

Level	Melt temperature	Shot size	Gas pressure	Gas delay
1	**1.92**	1.28	1.4	1.07
2	1.66	**1.67**	**1.64**	1.65
3	0.78	1.43	1.34	**1.66**
Delta	1.14	0.4	0.31	0.59
Portion	47%	16%	13%	24%
Rank	1	3	4	2

Table 12. Process parameter rank of significance on RWT for GAPIM experiment with SSFP.

Level	Melt temperature	Shot size	Gas pressure	Gas delay
1	3.43	**3.69**	3.55	2.88
2	**3.94**	3.55	3.54	3.61
3	3.43	3.57	**3.72**	**4.33**
Delta	0.51	0.13	0.19	1.45
Portion	22%	6%	8%	64%
Rank	2	4	3	1

Table 11 and 12 identify the processing parameter ranks of significance on RWT for GAIM with PP, and GAPIM with SSPF, respectively. Table 11 shows that the melt temperature is the most significant parameter with a portion of 47% and the gas delay time is also significant parameter with a portion of 24% in GAIM. Compared to the results of gas penetration depth, the significance of melt temperature increased, while the significance of shot size decreased. It indicates that the melt flow properties and frozen layer have an effect on RWT more than the shot size. Table 12 shows that the gas delay time has the most significant effect on RWT with a portion of 64%, and the melt temperature has a portion of 22%. The gas delay time, which was the most significant parameter on gas penetration depth, still played an important role in RWT. The higher significance of gas delay time with SSPF than PP is due to the fast cooling in cavity wall, resulting in a thicker frozen layer.

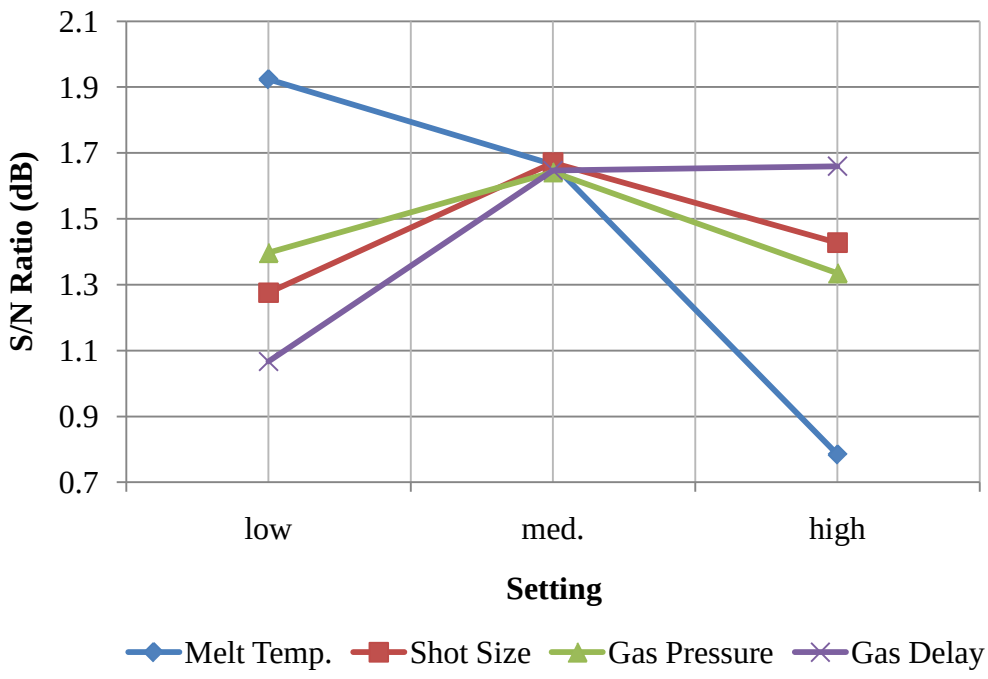

Figure 27. Main effects plots for experiment on RWT of GAIM with PP.

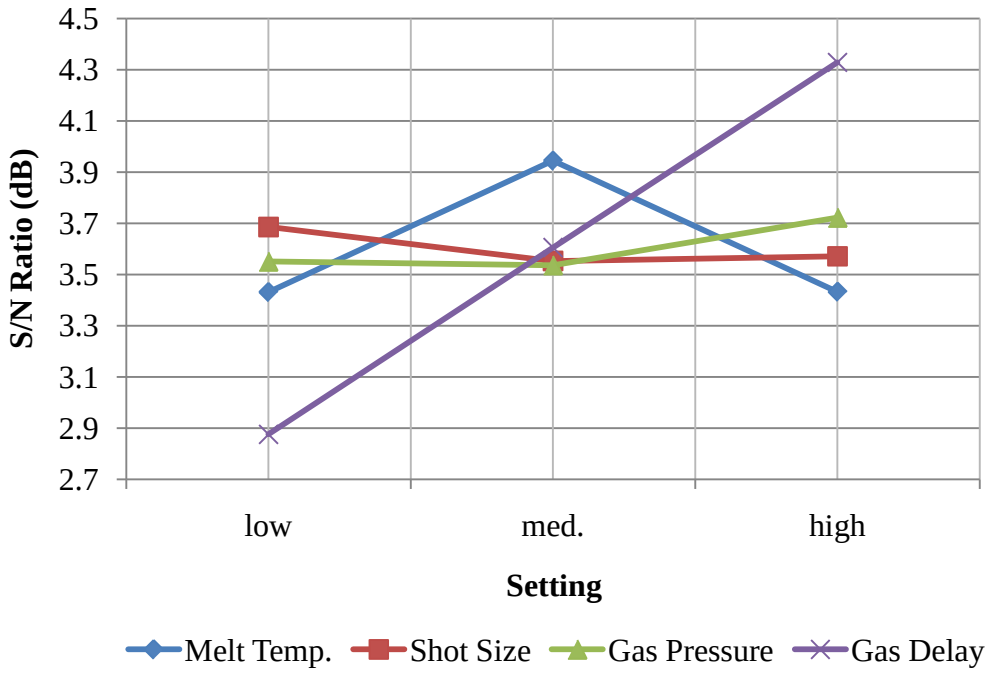

Figure 28. Main effects plots for experiment on RWT of GAPIM with SSPF.

Figure 27 and 28 illustrates the main effects plots for RWT in the experiments with PP and SSPF. In GAIM with PP, low melt temperature and high delay time yield the highest RWT. In GAPIM with SSPF, high gas delay time results in a significantly larger RWT. This is mainly due to the thickness of the frozen layer increase with the gas delay time increase. This result also agrees with published research [31, 34, 36] in plastics. Particularly, the high thermal conductivity of the feedstock used lead to the faster solidification of frozen layer in the cavity during the gas delay period. On the other hand, there were no significant effects of shot size and gas pressure on the RWT.

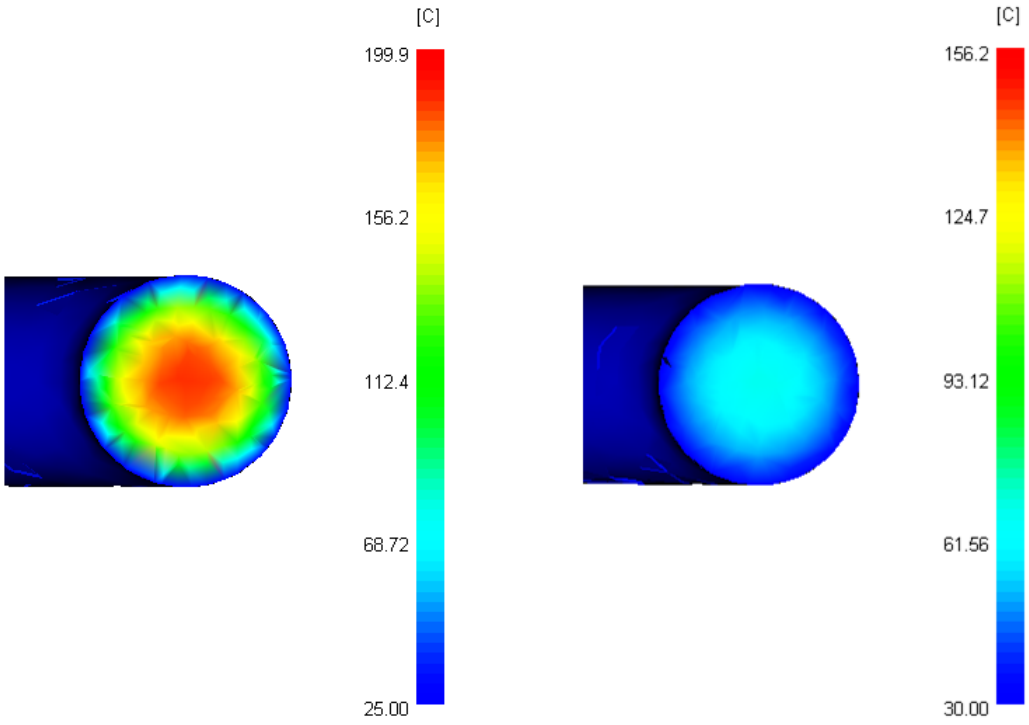

(a) PP (b) SSPF

Figure 29. Temperature distribution of melt cores after completion of filling stage.

Figure 29 shows the cross sections of the molded parts from the results of the AMI simulation runs indicating the temperature changes in the cavity, and the dramatic temperature difference between PP and SSPF can be observed. These cross sections represented 8.01 seconds in GAIM and 6.45 seconds in GAPIM after injection started. It is obvious that the SSPF solidifies much faster than PP which explains the delay time and higher portion in GAPIM than in GAIM. However, the simulation results using Al cavity and SLA cavity (Lee et. al. [8]) showed no differences which indicated AMI simulation failed to consider the effect of thermal conductivity differences between SLA and Al.

Effect of Mold Temperature on Gas Penetration Depth and RWT

Simulation Result

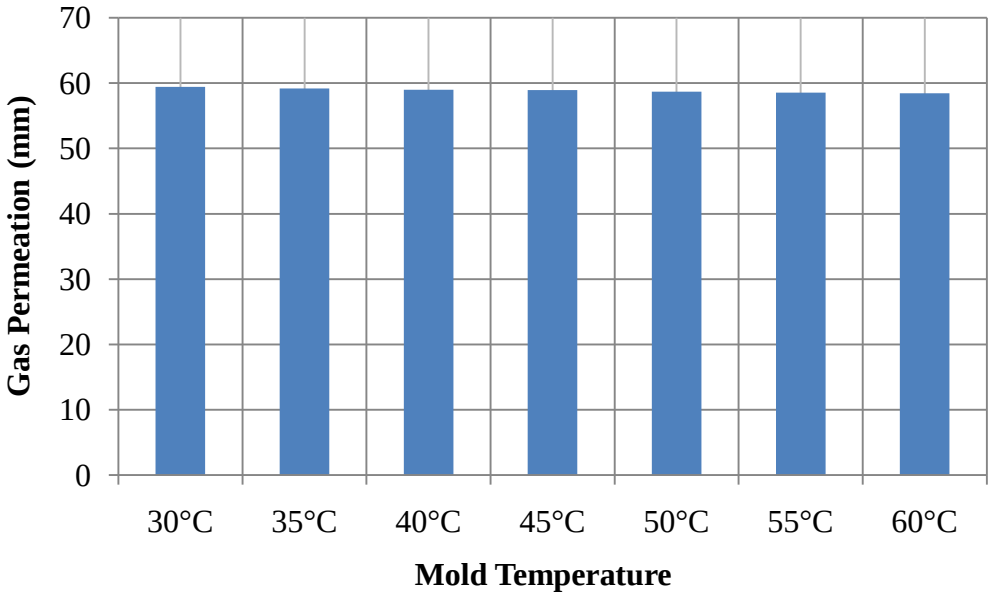

Figure 30. Gas penetration depth versus mold temperature for simulation of GAPIM with SSPF.

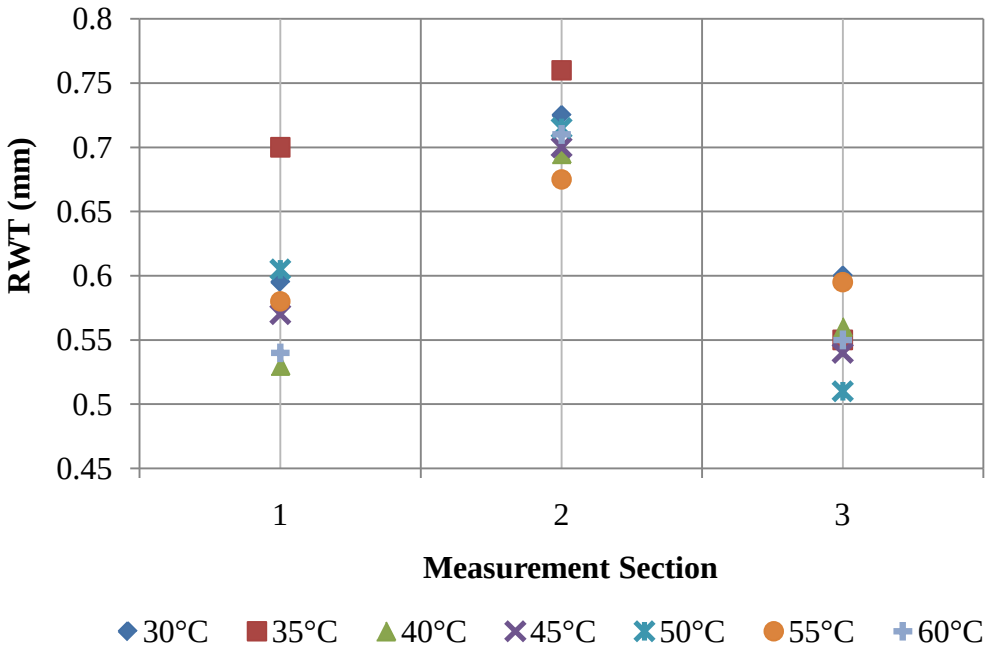

Figure 31. RWT at each section for simulation of GAPIM with SSPF.

Figure 30 shows the effect of mold temperature on the gas penetration depth in simulation runs and that the gas penetration depth decreases as the mold temperature increases. Figure 31 shows RWT at each section for simulation runs of GAPIM in various mold temperatures. It indicates that RWT is not controllable by changing mold temperature input data in simulation runs.

Experiment Result

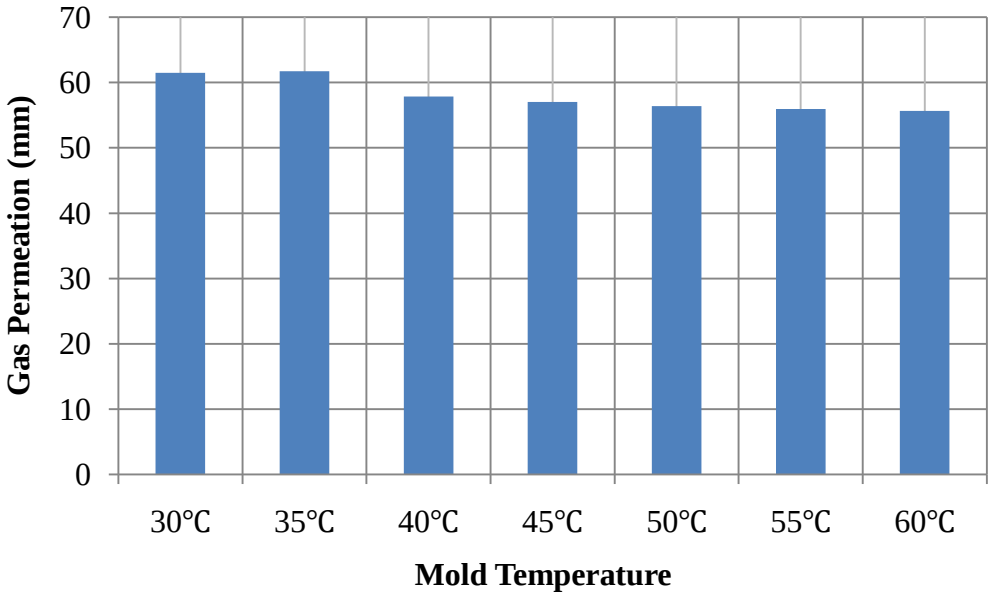

Figure 32. Gas penetration depth versus mold temperature for experiment of GAPIM with SSPF.

Figure 32 shows the effect of mold temperature on the gas penetration depth in the experiment and that the gas penetration depth decreases as the mold temperature increases even more obviously than the simulation result. This result agrees with Chau's study with plastics [37] and Michaeli's study with powder feedstock [7]. According to the previous studies, the RWT decreases as the mold temperature increases due to the

decrease of frozen layer during the injection stage, caused by the lower viscosity and slower cooling of the melt. As the frozen layer decreases, more melt of material is available to fill out the remaining volume of the cavity, and this leads to the lower gas penetration depth [33, 37].

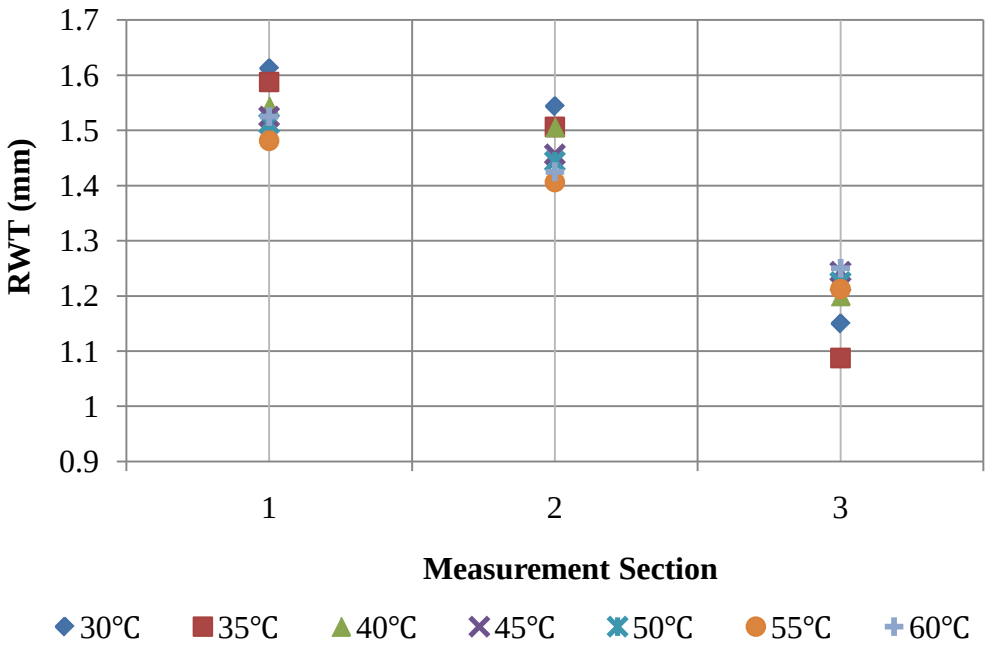

Figure 33. RWT at each section for experiment of GAPIM with SSPF.

Figure 33 shows the effect of the mold temperature on RWT at each section and it also shows that the RWT decreases as the mold temperature increases. When the mold temperature changed from 30 to 60°C, the RWT changed from 1.61 to 1.53mm in section 1, and from 1.54 to 1.43mm in section 2. Since the gas penetration depth affected the RWT measurement for section 3, the effect of mold temperature on RWT in the section 3 was insignificant, while the significant changes of RWT over mold temperature changes were observed in the section 1 and 2.

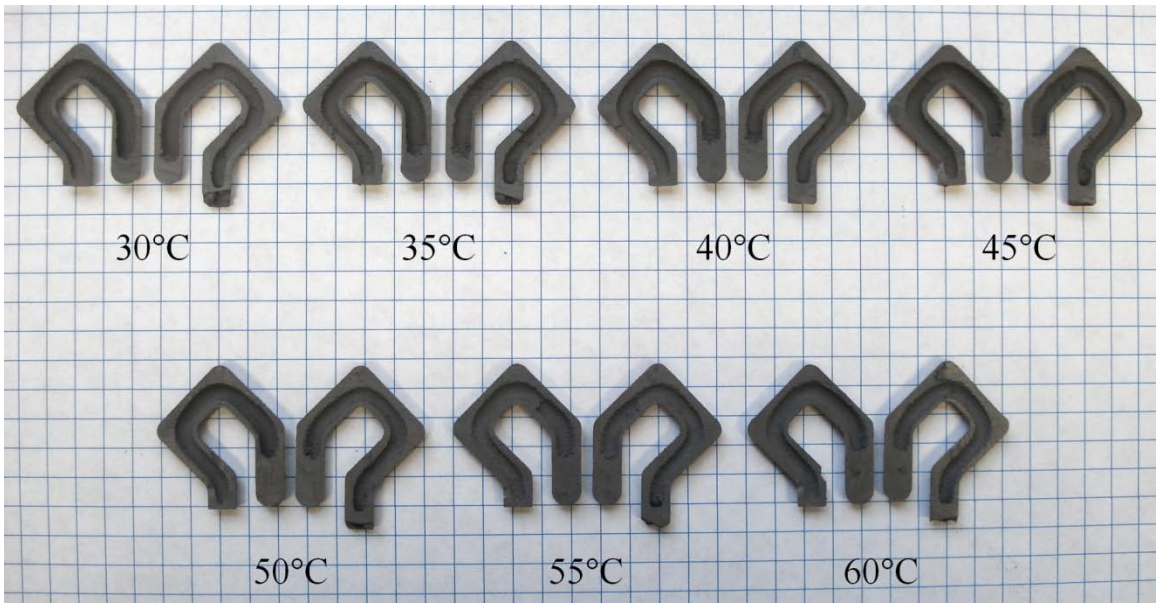

Figure 34. Samples fabricated under different mold temperature.

Figure 34 shows the samples fabricated under the various mold temperatures in the GAPIM experiment using SSPF. All parts show the excellent gas penetration with optimum surface finish. However, when the samples were split in halves to measure the gas penetration depth, bubble formation was observed. This is due to the gas penetration during the gas injection molding stage through the binder which is mostly wax and polymers, not through the metal powder. Then the bubble was formed during the degassing stage. In the case of the polymer, bubbling was not significantly obvious since the gas penetrated through the plastic evenly and the phase separations were not observed since the molded plastic is in a homogeneous stage. On the other hand, in GAPIM, there was the clear phase separation existed between the binder and metal powder. This heterogeneous system makes the bubbling become obvious.

CHAPTER V

CONCLUSIONS

This research reports the effects of processing parameters on gas penetration depth and Residual Wall Thickness (RWT) with an Aluminum (Al) cavity insert. While the simulation from Autodesk Moldflow Insight (AMI) effectively predicted the gas penetration patterns in Gas-Assisted Injection Molding (GAIM) with Polypropylene (PP), it was not sensitive to the gas pressure and gas delay time in Gas-Assisted Powder Injection Molding (GAPIM) with Stainless Steel Powder Feedstock (SSPF). The AMI simulation also failed to consider the effect of thermal conductivity differences between Stereolithography (SLA) and Al cavities.

In the GAIM experiment with PP, there was no significant difference of gas penetration depth between the SLA cavity and Al cavity. However, in the GAPIM experiment with SSPF, the significance of gas delay time was relatively higher in the Al cavity than in the SLA cavity. This is because the thermal conductivity of the Al cavity (190 W/m-C) is considerably higher than that of the SLA cavity (1.47 W/m-C), showing that cooling is much faster in the Al cavity. Generally, the gas channels were developed better with the Al than the SLA cavity inserts. The effect of gas delay time also showed a difference between GAIM and GAPIM. The gas delay time had higher significance in the GAPIM experiment than in GAIM. This difference is mainly due to the higher thermal diffusivity of SSPF as compared to PP. The optimum gas penetration depth was obtained

in the processing conditions identified by high gas delay time, low melt temperature, and low shot size. Gas pressure was an insignificant parameter in all simulations and experiments.

The effect of the processing conditions on RWT was also considered. For the GAIM experiment, melt temperature was the most significant parameter and gas delay time was next. Low melt temperature and high gas delay time yield the highest RWT. The low melt temperature causes increases in viscosity of the material and more melt accumulates on the cavity wall corresponding to less transfer of melt from the melt layer to downstream of the gas front. This allows less resistance to gas penetration into the cavity. Accordingly, the gas penetration depth and RWT also increase with the thick frozen layer. For the GAPIM experiment, gas delay time was the most significant parameter and melt temperature was next. The significance of gas delay time shows that cooling from the surface of the cavity is more sensitive to gas penetration depth and RWT in GAPIM. As the gas delay time increases more time for heat transfer is provided to solidify the injected feedstock on the cavity wall. This directly affects the RWT and associated thickness of the frozen layer. While the RWT was not in control in the GAPIM experiment, RWT was thicker and more uniform with an Al cavity than with the previous SLA cavity study.

As an additional processing parameter, mold temperature, which is known as one of the significant parameters, was varied to find the effect on gas penetration depth and RWT. An increase in mold temperature yields a decrease in gas penetration depth and RWT. This also can be explained by the frozen layer in the cavity wall. If the mold temperature is low, the viscosity of the injected material will increase. The high viscosity

causes more accumulation of melt on the cavity wall and less melt flows from the melt layer to downstream of the gas front giving low resistance to gas penetration. The accumulation also leads to a thicker frozen layer in the cavity wall resulting in high RWT. With the higher mold temperature, the viscosity increase is lower during the injection stage of SSPF. The lower viscosity increase causes more translation of melt from melt layer to downstream of the gas front. The lower accumulation of melt yields a thinner frozen layer and a low RWT. The increased amount of melt downstream of the gas front also interrupts more gas penetration. This phenomenon is observed in the GAPIM experiment with SSPF and is the same as that of plastics.

REFERENCES

[1] German, R.M., & Bose, A. (1997). Injection molding of metal and ceramics. Metal Powder Industries Federation, Princeton, NJ.

[2] Bloemacher, M., & Weinand, D. (1997). Catamold™: a new direction for powder injection molding. *Journal of Materials Processing Technology*, 63(1-3), 918-922.

[3] Vervoort, P.J., Vetter, R., & Duszczyk, J. (1996). Overview of powder injection molding. *Advanced Performance Materials*, 3(2), 121-151.

[4] Malloy, R. A. (1994). Plastic part design for injection molding: an introduction. Hanser, Munich.

[5] Heim, H.P., & Potente, H. (2001). Specialized molding techniques. William Andrew Publishing, Norwich, NY, 73-78.

[6] Qingfa, L. (2000). Gas-assisted PIM. SIMTech Technical Report.

[7] Michaeli, W., & Hopmann, C. (2000). New perspectives for ceramic injection molding with gas injection. *Advanced Engineering Materials*, 2(12), 827-832.

[8] Lee, K., De Hoyos, M., Ahn, S., Nambiar, R., Gonzalez, M.A., Park, S.J., & German, R.M. (2010). Gas-assisted powder injection molding: a study on the effect of processing variables on gas penetration. *Powder Technology*, 200(3), 128-135.

[9] Nambiar, R. V., Lee, K. H., & Nagarajan, D. (2007). Stereolithography mold life extension using gas-assisted injection.

[10] German, R.M. (2008). PIM breaks the $1 bn barrier. *Metal Powder Report*, 63(3), 8-10.

[11] Berginc, B., Kampus, Z., & Sustarsic, B. (2006). The influence of MIM and sintering-process parameters on the mechanical properties of 316L SS. *Materials and Technology*, 40(5), 193-198.

[12] Liu, Z.Y., Loh, N.H., Tor, S.B., Khor, K.A., Murakoshi, Y., Maeda, R., & Shimizu, T. (2002). Micro-powder injection molding. *Journal of Materials Processing Technology*, 127(2), 165-168.

[13] Berginc, B., Brezocnik, M., Kampus, Z., & Sustarsic, B. (2009). A numerical simulation of metal injection moulding. *Materials and Technology*, 43(1), 43-48.

[14] Baojun, Z., Xuanhui, Q., & Ying, T. (2002). Powder injection molding of WC-8%Co tungsten cemented carbide. *International Journal of Refractory Metals and Hard Materials*, 20(5-6), 389-394.

[15] Rak, Z.S. (1999). New trend in powder injection moulding. *Powder Metallurgy and Metal Ceramics*, 38(3-4), 126-132.

[16] Piotter, V., Mueller, T., Plewa, K., & Prokop, J. (2010). Manufacturing of complex-shaped ceramic components by micropowder injection molding. *International Journal of Advanced Manufacturing Technology*, 46(1-4), 131-134.

[17] Karatas, C., Sozen, A., Arcaklioglu, E., & Erguney, S. (2008). Investigation of mouldability for feedstocks used powder injection moulding. *Materials and Design*, 29(9), 1713-1724.

[18] Ruprecht, R., Gietzelt, T., Muller, K., Piotter, V., & Haubelt, J. (2002). Injection molding of microstructured components from plastics, metals and ceramics. *Microsystem Technologies*, 8(4-5), 351-358.

[19] Urval, R., Lee, S., Atre, S.V., Park, S.-J., & German, R.M. (2008). Optimisation of process conditions in powder injection moulding of microsystem components using a robust design method: part I. primary design parameters. *Powder Metallurgy*, 51(2), 133-142.

[20] Parvez, M.A., Ong, N.S., Lam, Y.C., & Tor, S.B. (2002). Gas-assisted injection molding: the effects of process variables and gas channel geometry. *Journal of Materials Processing Technology*, 21(1), 27-35.

[21] Ilinca, F., & Hetu, J.F. (2003). Three-dimensional simulation of multi-material injection molding: application to gas-assisted and co-injection molding. *Polymer Engineering and Science*, 43(7), 1415-1427.

[22] Li, Q., Wang, X., Shen, C., Jiang, J., & Hou, S. (2007). Influence of processing parameters on shrinkage of LDPE parts in gas-assisted injection molding. ANTEC, 625-629.

[23] Polynkin, A., Pittman, J.F.T., & Sienz, J. (2007). Approximate prediction of gas core geometry in gas assisted injection molding using a short cut method. *Polymer Engineering and Science*, 47(5), 713-720.

[24] Lee, K. H. A study of fingering phenomena in the gas-assisted injection molding process: the effects of processing variables and the fluidity ratio. PhD. Dissertation, U. Mass., Lowell.

[25] Avery, J. (2001). Gas-assist injection molding: principles and applications. Hanser, Munich.

[26] Poslinski, A.J., Oehler, P.R., & Stokes, V.K. (1995). Isothermal gas-assisted displacement of viscoplastic liquids in tubes. Polymer Engineering and Science, 35(11), 877-892.

[27] Chen, S.C., Hsu, K.S., & Huang, J.S. (1995). Experimental study on gas penetration characteristics in a spiral tube during gas-assisted injection molding. *Industrial and Engineering Chemistry Research*, 34(1), 416-420.

[28] Yang, S.Y., & Chou, H.L. (2002). Study on the residual wall thickness at dimensional transitions and curved sections in gas-assisted molded circular tubes. *Polymer Engineering and Science*, 42(1), 111-119.

[29] Lin, K.Y., Chang, F.A., & Liu, S.J. (2009). Using differential mold temperatures to improve the residual wall thickness uniformity around curved sections of fluid assisted injection molded tubes. *International Communications in Heat and Mass Transfer*, 36(5), 491-497.

[30] Bryce, D.M. (1997). Plastic injection moulding: material selection and product design fundamentals, Society of Manufacturing Engineers, Dearborn, MI.

[31] Ong, N.S., Lee, H.L., & Parvez, M.A. (2001). Influence of Processing Conditions and Part Design on the Gas-Assisted Injection Molding Process. *Advances in Polymer Technology*, 20(4), 270-280.

[32] Yang, S.Y., Lin, C.T., & Chang, J.H. (2003). Secondary gas penetrations in ribs during full-shot gas-assisted injection molding. *Advances in Polymer Technology*, 22(3), 225-237.

[33] Gas-injection moulding with DuPont engineering polymer. DuPont Technical Report.

[34] Carrillo, A.J., & Isayev, A.I. (2009). Birefringence in gas-assisted tubular injection moldings: simulation and experiment. *Polymer Engineering and Science*, 49(12), 2350-2373.

[35] Van Hoye, W., Callewaert, K., Hick, R., Vermeersch, R., Beeckman, E., Emmerechts, C., & Casteleyn, E. (2005). Fabrication of thin cavities with gas assisted injection moulding: experiments and simulations. 1-8.

[36] Polynkin, A., Pittman, J.F.T., & Sienz, J. (2005). Gas assisted injection molding of a handle: three-dimensional simulation and experimental verification. *Polymer Engineering and Science*, 45(8), 1049-1058.

[37] Chau, S.W. (2008). Three-dimensional simulation of primary and secondary penetration in a clip-shaped square tube during a gas-assisted injection molding process. *Polymer Engineering and Science*, 48(9), 1801-1814.

APPENDIX A

APPENDIX A

MATERIAL PROPERTIES

Polypropylrene

Table A1. Recommended processing molding window.

Parameter	Value
Mold Surface Temperature	40°C
Mold Temperature Range	min = 20°C, max = 60°C
Melt Temperature	240°C
Melt Temperature Range	min = 220°C, max = 260°C
Absolute Maximum Melt Temperature	280°C
Ejection Temperature	101°C
Maximum Shear Stress	0.25 MPa
Maximum Shear Rate	100,000 1/s

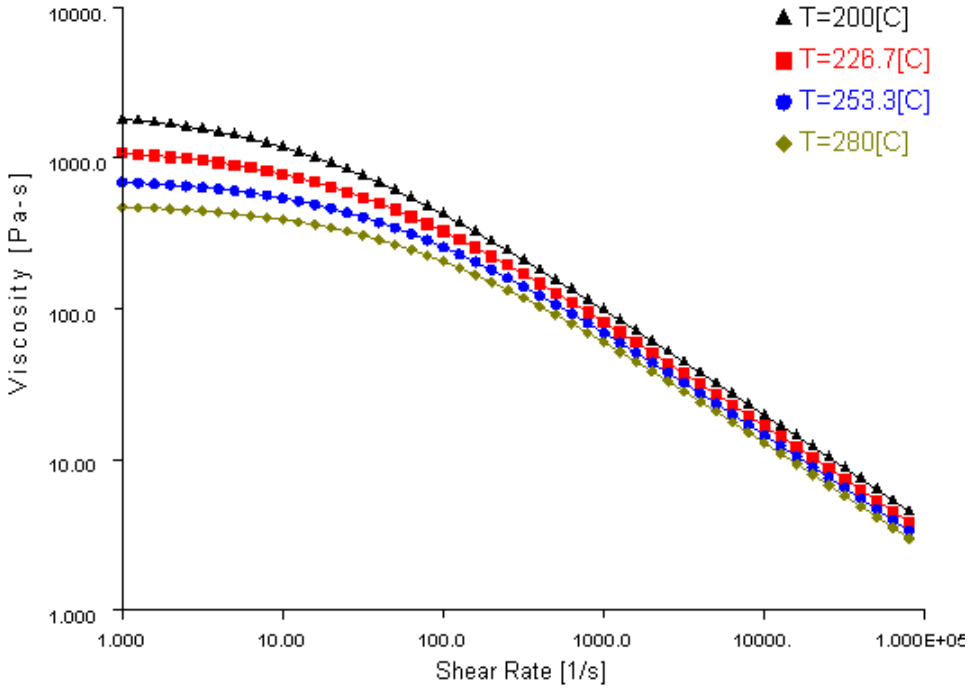

Figure A1. 13T10Acs279 rheological data.

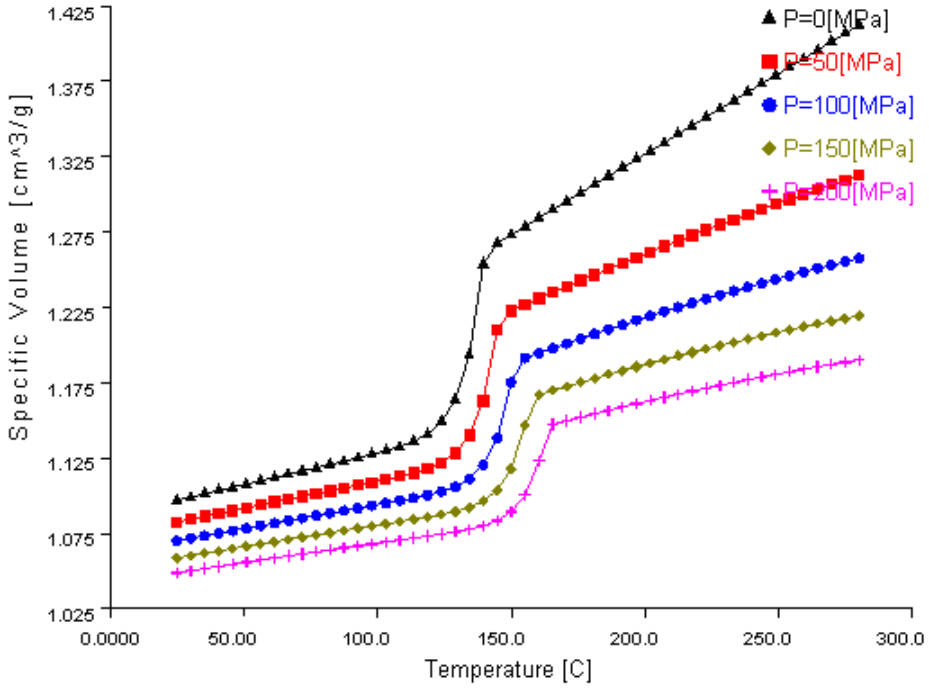

Figure A2. 13T10Acs279 PVT data.

Table A2. Curve fitting coefficients of cross WLF equation.

Rheological (cross WLF equation)
n = 0.2751
Tau = 24200 Pa
D1 = 4.66e+12 Pa-s
D2 = 263.15 K
D3 = 0 K/Pa
A1 = 26.12
A2 = 51.6 K
T Tran. = 111°C

Table A3. Thermal properties.

Thermal Data	
Specific Heat	
Temp. = 240°C	Specific Heat = 2740 J/kg-C
Thermal Conductivity	
Temp = 240°C	Thermal Conductivity = 0.164 W/m-C

Table A4. Curve fitting coefficients for the two domain Tait model.

PVT Properties (two domain Tait model)
Melt density = 0.72828 g/cm^3
Solid density = 0.89163 g/cm^3
b5 = 388.75 K
b6 = 2.2×10^{-7} K/Pa
b1m = 0.00125 m^3/kg
b2m = 9.986×10^{-7} m^3/kg-K
b3m = 6.94565e+7 Pa
b4m = 0.003782 1/K
b1s = 0.001147 m^3/kg
b2s = 2.85e-7 m^3/kg-K
b3s = 1.64072e+8 Pa
b4s = 0.002712 1/K
b7 = 0.0001026 m^3/kg
b8 = 0.119 1/K
b9 = 3.01e-8 1/Pa

SUS316L STAINLESS STEEL FEEDSTOCK

Table A5. Recommended processing molding window.

Parameter	Value
Mold Surface Temperature	30°C
Mold Temperature Range	min = 30°C, max = 60°C
Melt Temperature	130°C
Melt Temperature Range	min = 120°C, max = 160°C
Absolute Maximum Melt Temperature	165°C
Ejection Temperature	50°C
Maximum Shear Stress	0.25 MPa
Maximum Shear Rate	100,000 1/s

Table A6. Curve fitting coefficients of cross WLF equation.

Rheological (cross WLF equation)
n = 0.18
Tau = 637,000 Pa
D1 = 74,000 Pa-s
D2 = 326 K
D3 = 0 K/Pa
A1 = 16.5
A2 = 326 K
T Tran. = 52.84°C

Table A7. Curve fitting coefficients for the two-domain Tait model .

PVT Properties (two-domain Tait model)
Melt density = 7.76 g/cm^3
Solid density = 7.76 g/cm^3
b5 = 345 K
b6 = 1.99×10^{-7} K/Pa
b1m = 0.0002334 m^3/kg
b2m = 1.156×10^{-7} m^3/kg-K
b3m = 2.94×10^{8} Pa
b4m = 0.004689 1/K
b1s = 0.000219 m^3/kg
b2s = 7.716×10^{-8} m^3/kg-K
b3s = 1×10^{9} Pa
b4s = 0.01 1/K
b7 = 1.446×10^{-5} m^3/kg
b8 = 0.03388 1/K
b9 = 9.328×10^{-9} 1/Pa

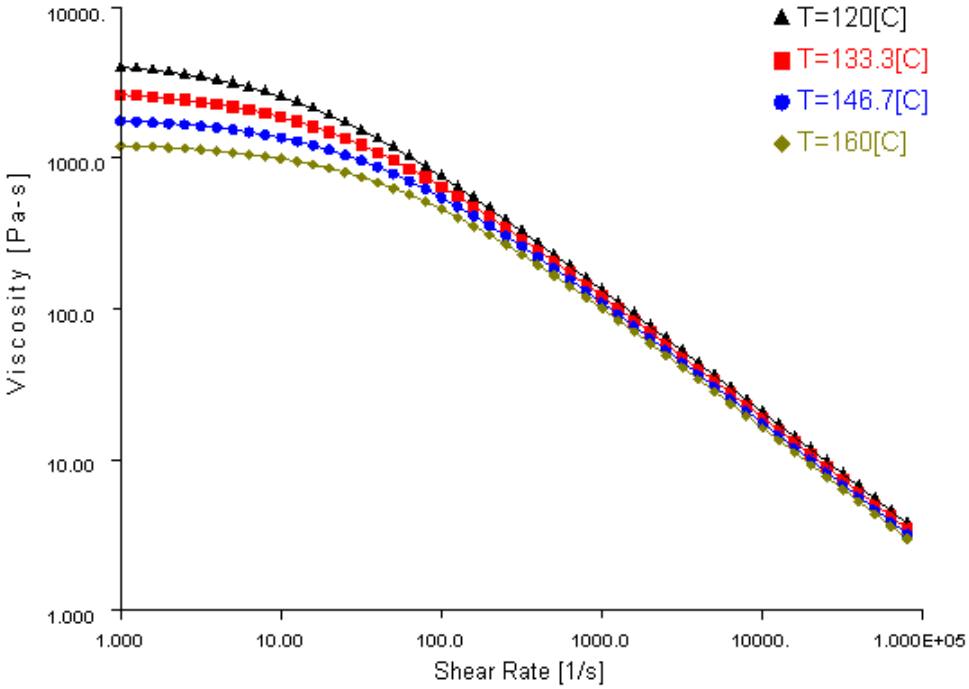

Figure A3. Cetatech SUS316L rheological data.

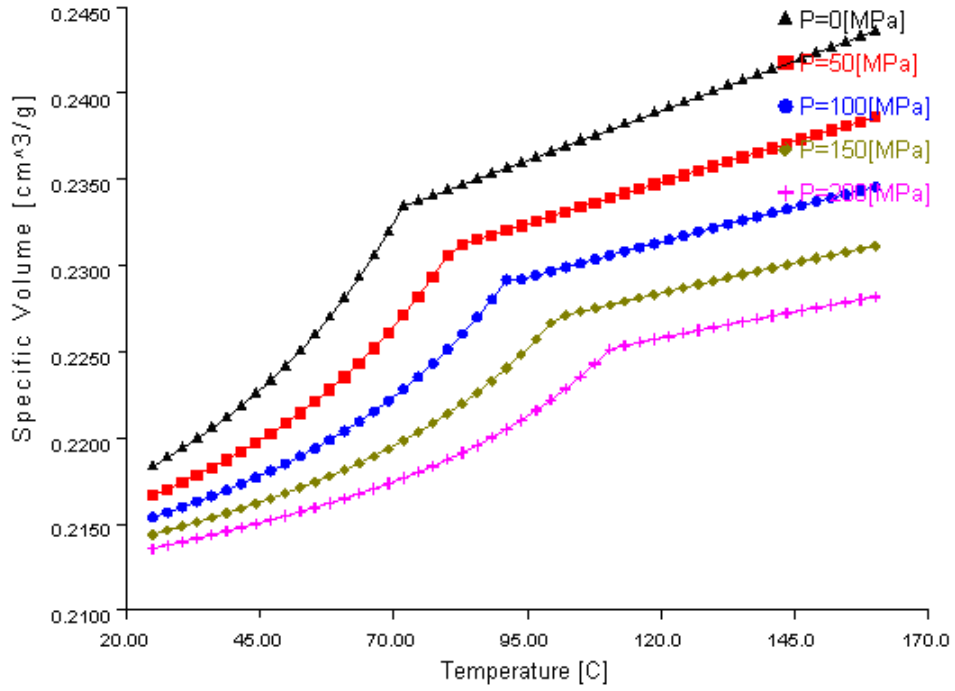

Figure A4. Cetatech SUS316L PVT data.

Table A8. Thermal Properties.

Thermal Data	
Specific Heat	
Temp. = 130°C	Specific Heat = 685 J/kg-C
Thermal Conductivity	
Temp = 130°C	Thermal Conductivity = 1.84 W/m-C

BIOGRAPHICAL SKETCH

Donghan Kim was born on March 9, 1980 in the city of Pusan in South Korea. He received the bachelor of Polymer Engineering from Pukyoung National University in 2007. During the bachelor's course, he served in the army for two years in South Korea. He has completed the master's course in Manufacturing Engineering at the University of Texas Pan-American.